

8. Spectroscopic Studies of the Electronic Structure

Zbigniew M. Stadnik

8.1 Introduction

The discovery of an icosahedral Al-Mn alloy by Shechtman et al. (1984) extended the dichotomous division of solids into either crystalline or amorphous by introducing the notion of quasiperiodic crystals, or quasicrystals (QCs). This new form of matter has a long-range *quasiperiodic* order and long-range orientational order associated with the classically forbidden fivefold (icosahedral), eightfold (octagonal), tenfold (decagonal), and 12-fold (dodecagonal) symmetry axes. The majority of known QCs are either icosahedral (*i*) or decagonal (*d*) alloys. A few known octagonal and dodecagonal alloys cannot be produced yet in sufficient quantity to allow studies of their physical properties. A central problem in condensed matter physics is to determine whether quasiperiodicity leads to physical properties significantly different from those of crystalline and amorphous materials.

The electronic structure of solids determines many of their fundamental physical properties. Therefore, experimental techniques which probe this structure directly are among the most important tools for understanding the microscopic properties of solids. Among these techniques, photoemission spectroscopy (PES) (Cardona and Ley 1978, Ley and Cardona 1979, Mahlhorn 1982, Hüfner 1996), which probes the density of states (DOS) below the Fermi level E_F , and inverse photoemission spectroscopy (IPES) and electron energy-loss spectroscopy (EELS) (Fuggle and Inglesfield 1992), which probe the DOS above E_F , are the most powerful in studies of the electronic structure of solids. These electronic states can be also probed, respectively, with soft-x-ray-emission (SXE) and soft-x-ray-absorption (SXA) spectroscopies (Agarwal 1991, Fuggle and Inglesfield 1992). Both the occupied and unoccupied DOS can also be investigated with tunneling spectroscopy (TS) (Wolf 1985, Stroscio and Kaiser 1993). The spectroscopies mentioned above were mainly used in studies of the DOS in QCs. In this chapter, the results based on these spectroscopies are critically reviewed and compared with the theoretical predictions.

This chapter is organized as follows. The main theoretical predictions of the electronic structure of QCs are briefly reviewed in Sect. 8.2. These predictions are discussed in detail in Chaps. 6 and 7. Spectroscopic results on the electronic structure of *i* and *d* QCs are presented in Sect. 8.3. Possible reasons for some discrepancies between theory and spectroscopic data are

also discussed. Possible unique features of the electronic structure of QCs are discussed in Sect. 8.4. Section 8.5 attempts to assess the influence of quasiperiodicity on the physical properties of QCs. Concluding remarks and some suggestions for future work are made in Sect. 8.6.

8.2 Theoretical Predictions

8.2.1 Pseudogap in the Density of States

One of the first questions posed after the discovery of QCs was the following: why nature would prefer quasiperiodic to periodic order in some alloys? It was soon pointed out, based on the observation that *i* alloys form at compositions with a specific electron-per-atom ratio, e/a , for which the relation $Q = 2k_F$ (Q is the magnitude of the reciprocal lattice vector and k_F is the radius of the Fermi sphere) is satisfied, that these alloys are the Hume-Rothery phases (Bancel and Heiney 1986, Tsai et al. 1989a, 1989b, Inoue et al. 1990). This was supported by the results of calculations within the nearly-free-electron approximation for models of *i* alloys (Friedel and Dénoyer 1987, Smith and Ashcroft 1987, Vaks et al. 1988, Friedel 1988, 1992). For the compositions at which the *i* alloys form, the Fermi surface-effective Brillouin zone interaction results in a minimum of the DOS(E_F) (a “pseudogap”). Modern band-structure calculations carried out for approximants (complex crystalline alloys close in composition and with a local structural similarity to QCs) to *i* alloys do indeed predict the existence of a structure-induced pseudogap at E_F (see Figs. 6.6–6.11 in Chap. 6 and Figs. 7.13, 7.14, and 7.16 in Chap. 7) in a number of *i* alloys (Fujiwara 1989, Fujiwara and Yokokawa 1991, Hafner and Krajčí 1992, 1993, Windisch et al. 1994, Trambly de Laissardière and Fujiwara 1994a, Krajčí et al. 1995, Dell’Acqua et al. 1997, Hennig and Teichler 1997, Krajčí and Hafner 1998). Theory thus predicts that a Hume-Rothery-type electronic mechanism is mainly responsible for the stabilization of *i* alloys.

Fewer approximants to *d* alloys are known. Therefore electronic structure calculations are available only for Al-Co-Cu, Al-Pd-Mn, Al-Fe, and Al-Mn *d* alloys. The first such band-structure calculations (Trambly de Laissardière and Fujiwara 1994b) made for the *d* approximant $\text{Al}_{60}\text{Co}_{14}\text{Cu}_{30}$, which was based on the Burkov model (Burkov 1991), predicted a broad Hume-Rothery-like pseudogap at E_F (see Fig. 6.11 in Chap. 6 and Fig. 7.14 in Chap. 7). However, calculations for several variants of the Burkov model showed (Sabiryanov and Bose 1994, Sabiryanov et al. 1995) that there is no pseudogap, and consequently that the *d*-Al-Co-Cu alloys are not stabilized by the Hume-Rothery mechanism. In another theoretical study Haerle and Kramer (1998) showed that the location of the transition metal (TM) atoms is crucial for the presence or absence of the pseudogap in the *d*-Al-Co-Cu system. The presence of a pseudogap was predicted in detailed band-structure calculations by Krajčí et al. (1997a) who argued that the Co and Cu *d*-band

shifts are important for the stabilization of the d -Al-Co-Cu phase. These contradictory theoretical predictions with regard to the presence of a pseudogap in the d -Al-Co-Cu system probably result from many possible variants of the Burkov model.

Band-structure calculations for approximants to the d -Al-Pd-Mn system predict (Krajčí et al. 1996, Krajčí et al. 1997b) that a structure-induced pseudogap exists only in the Al band and stress the importance of the sp - d hybridization in its formation. The DOS calculated for approximants to the Al-Fe (Fujiwara and Yokokawa 1991) and Al-Mn (Fujiwara 1997) d phases predict, respectively, the presence of a pseudogap and a very deep pseudogap.

8.2.2 Fine Structure of the Density of States

The DOS of i alloys is very unusual in that it consists of many very fine spiked peaks with a width of about 10 meV. This DOS spikiness results from the multiplicity of dispersionless bands. Based on band-structure calculations performed for approximants to i alloys, such a fine structure has been predicted for Al-Cu-Li (Fujiwara and Yokokawa 1991), Al-Mg-Li (Dell'Acqua et al. 1997), Al-Zn-Mg (Hafner and Krajčí 1992, Windish et al. 1994), Al-Mn (Fujiwara 1989), Al-Cu-Fe (Trambly de Laissardière and Fujiwara 1994a), Al-Pd-Mn (Krajčí et al. 1995), Al-Pd-Re (Krajčí and Hafner 1998), and Ti-TM (Krajčí and Hafner 1994, Hennig and Teichler 1997) i alloys. It has been argued (Trambly de Laissardière and Fujiwara 1994a) that the DOS spikiness is augmented by the presence of the TM atoms in the i alloys. The DOS spikiness is predicted even for simple models in which quasiperiodic order is introduced (Roche et al. 1997).

The presence of the DOS spikiness may explain the unusual sensitivity of the electrical conductivity σ of i alloys to slight changes in their composition. Such changes shift the position of E_F , which results in a dramatic change of the DOS(E_F), and consequently of the value of σ (Fujiwara et al. 1993). The unusual composition and temperature dependences of other transport properties, such as the Hall conductivity and the thermoelectric power, can be also qualitatively explained (Fujiwara et al. 1993) by the presence of the DOS fine structure.

The DOS spikiness is predicted to be also present in d alloys (Fujiwara and Yokokawa 1991, Trambly de Laissardière and Fujiwara 1994b, Sabiryanov and Bose 1994, Krajčí et al. 1997a, Haerle and Kramer 1998). However, it is attenuated, in comparison to that in i alloys, by the effect of the periodic direction (Trambly de Laissardière and Fujiwara 1994b). It thus appears that the predicted fine structure of the DOS is important for explaining unusual dependences on the composition and temperature of some electronic transport properties of QCs.

The fine structure of the DOS has been calculated with different techniques for various approximant systems and is therefore regarded as an intrinsic characteristic of the electronic structure of QCs. However, a concern

has been expressed that it may be an artifact resulting from the insufficient computational precision used in the calculations (Haerle and Kramer 1998).

8.3 Experimental Results

In this section an overview of the spectroscopic data on the DOS below and above E_F is presented. An experimental evidence for the presence of the predicted pseudogap and of the DOS spikiness in i and d QCs is discussed.

8.3.1 s, p -Bonded Icosahedral Alloys

The first stable i alloy was discovered in the Al-Cu-Li system (Dubost et al. 1986). There is an intermetallic compound in this system, called the R phase, which is the 1/1 approximant to the i -Al-Cu-Li alloy. The electronic structure calculations carried out for this approximant (Fujiwara and Yokokawa 1991) revealed the presence of a pseudogap in the DOS at E_F . This was confirmed later by Windisch et al. (1994) who found that the DOS minimum occurs just 30 meV below E_F . Calculations for higher-order approximants, up to a 8/5 approximant (Windisch et al. 1994), confirmed that a deep, structure-induced pseudogap slightly below E_F (Fig. 7.13 in Chap. 7) is a generic property of the i -Al-Cu-Li alloys.

PES spectra of the i -Al-Cu-Li alloy and the R phase measured at photon energies $h\nu = 100$ and 40 eV, with an energy resolution respectively of 0.7 and 0.3 eV, are shown in Fig. 8.1a. The measured PES intensity is the weighted average of the local partial DOS, with the weight proportional to the $h\nu$ -dependent photoionization cross section, σ_{ph} (Stadnik et al. 1995a). A strong feature at the binding energy (BE) of about -4.1 eV (the minus sign indicates the energies below E_F which is assigned the value of 0.0 eV) is predominantly due to the Cu $3d$ -derived states. This conclusion is based on the fact that σ_{ph} of Cu $3d$ orbitals is about two orders of magnitude larger than σ_{ph} of Al and Li sp orbitals and on its weak dependence on $h\nu$ in the $h\nu$ range 40–100 eV (Yeh 1993). Since the values of σ_{ph} of Al and Li sp orbitals decrease by a factor of about three in the $h\nu$ range 40–100 eV (Yeh 1993), an enhancement of the broad feature in the BE region between 0 and -3 eV in the PES spectrum measured at $h\nu = 40$ eV (Fig. 8.1a) as compared to the feature in the $h\nu = 100$ eV spectrum shows that this feature is mainly of the Al and Li sp character.

A comparison between the PES spectra calculated (Windisch et al. 1994) on the basis of the DOS for the 5/3 (Fig. 7.13 in Chap. 7) and 1/1 approximants, and the experimental PES spectra from Fig. 8.1a, is presented in Fig. 8.1b. The position of the DOS peak due to the Cu $3d$ -like states at $BE \approx -3.2$ eV (Fig. 7.13 in Chap. 7) is different than the corresponding position in the experimental spectrum (Fig. 8.1a). This is due to the

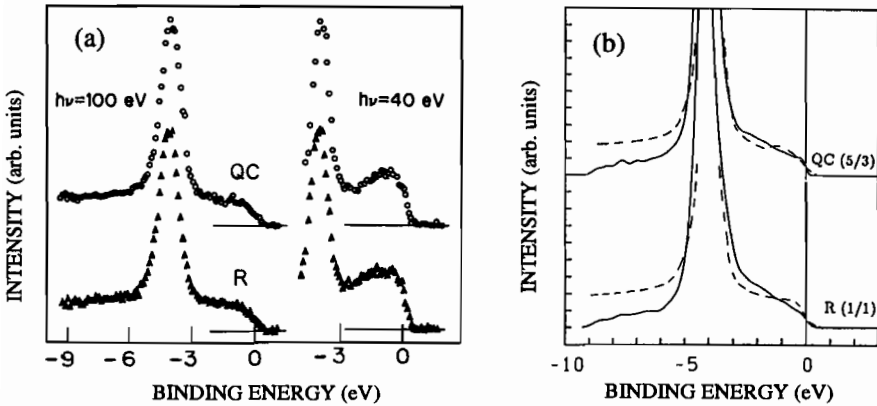


Fig. 8.1. (a) Valence bands of *i* QC $\text{Al}_{55}\text{Li}_{35.8}\text{Cu}_{9.2}$ and *R* phase $\text{Al}_{54}\text{Li}_{36.8}\text{Cu}_{9.2}$ measured at $h\nu = 100$ and 40 eV. After Matsubara et al. (1991). (b) Comparison between the $h\nu = 100$ eV valence bands of *i* QC $\text{Al}_{55}\text{Li}_{35.8}\text{Cu}_{9.2}$ and *R* phase $\text{Al}_{54}\text{Li}_{36.8}\text{Cu}_{9.2}$ (broken lines) from (a) with the calculated PES spectra for a 5/3 approximant and *R* phase (solid lines). After Windisch et al. (1994).

fact that PES spectra involve excited-state eigenvalues, whereas calculated DOS involves ground-state energies (Knapp et al. 1979, Fuggle and Inglesfield 1992). For narrow *d*-band systems, a comparison between the theoretical and experimental PES spectra requires an inclusion of the self-energy correction in theoretical calculations. This correction was simulated (Windisch et al. 1994) by shifting the calculated Cu *d* DOS so as to match the position of the experimental Cu-3*d* peak (Fig. 8.1b). There is reasonable agreement between theory and experiment with respect to the positions and intensities of the main features of the total DOS. The discrepancies at the *BE*'s lower (more negative) than about -5 eV (Fig. 8.1b) are due to the fact that the experimental PES spectra were not corrected for the secondary-electron contribution (Stadnik et al. 1995a).

The experimental PES spectra of the *i*-Al-Cu-Li and its 1/1 approximant (Fig. 8.1a) are virtually the same, although after normalization of the Cu 3*d* intensity Matsubara et al. (1991) found that the PES intensity at E_F of the *i* phase is slightly smaller than that of the *R* phase. This agrees with the observation that the electronic specific heat coefficient γ , which is proportional to $\text{DOS}(E_F)$, is slightly smaller for the *i*-Al-Cu-Li phase than for the *R* phase (Mizutani et al. 1991).

The decrease of the experimental PES intensity towards E_F (Fig. 8.1a) is often interpreted as evidence for the existence of a pseudogap in the DOS at E_F . This is an overinterpretation of the experimental data. The PES technique probes the electronic states below E_F , but the pseudogap involves both occupied and unoccupied states. Thus, conclusive evidence for the existence of a pseudogap requires probing the electronic states both below and above

E_F . The only reliable conclusion that can be drawn from the PES intensity decrease towards E_F (Fig. 8.1a) is that it is indicative of the presence of a pseudogap around E_F . Similarly, interpreting the small value of γ found in many QCs as evidence for the existence of a DOS pseudogap at E_F is not justified as γ is a measure of the DOS at only one particular energy (E_F). A small value of γ for a given QC as compared, e.g., to that of Al metal is merely suggestive of the presence of a pseudogap at E_F in that QC, but does not prove its existence.

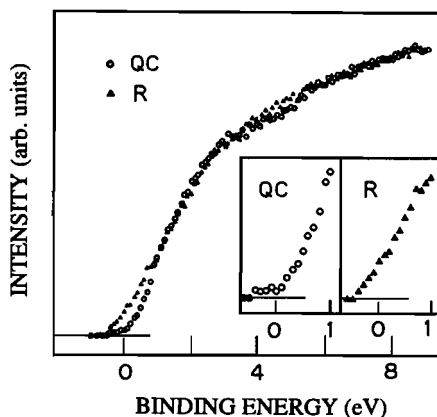


Fig. 8.2. IPES spectra of *i* QC $\text{Al}_{55}\text{Li}_{35.8}\text{Cu}_{9.2}$ and *R* phase $\text{Al}_{54}\text{Li}_{36.8}\text{Cu}_{9.2}$. The relative intensities have been normalized at the high-*BE* region. The insert shows the spectra close to E_F . After Matsubara et al. (1991).

A comparison between the IPES spectra of the *i*-Al-Cu-Li and *R* phases (Fig. 8.2) shows that the pseudogap is opening slightly above, rather than below E_F , and that it is shallower in the latter than in the former. A combination of PES and IPES spectra thus establishes that, as predicted by theory, there is a pseudogap in the DOS in the *i*-Al-Cu-Li alloy and the *R* phase, but slightly above, rather than below E_F . The difference between theory and experiment as to location of the minimum of the DOS is most probably due to the difference between the composition of the samples used in the experiment and that used in the calculations. This is based on the observation (Fujiwara and Yokokawa 1991) that the position of E_F in the Al-Cu-Li alloys shifts with the change of the Cu concentration.

Electronic structure calculations predict the presence of a pseudogap in the DOS at E_F for the stable Frank-Kasper phase $\text{Al}_{13}\text{Zn}_{36}\text{Mg}_{32}$ (the 1/1 approximant to the *i* phase) and for higher-order approximants to the *i* phase in the Al-Zn-Mg system (Hafner and Krajčí 1992, 1993). Such a pseudogap is also predicted (Fig. 6.9 in Chap. 6) for the 1/1 approximants in the $\text{Al}_x\text{Zn}_{60-x}\text{Mg}_{40}$ ($x = 15\text{--}22.5$) series (Mizutani et al. 1998). A slight

apparent decrease of the intensity in the x-ray photoelectron spectroscopy (XPS) valence bands of the 1/1 approximants $\text{Al}_x\text{Zn}_{60.5-x}\text{Mg}_{39.5}$ ($x = 20.5-45.5$) and the *i* QCs $\text{Al}_x\text{Zn}_{56-x}\text{Mg}_{44}$ ($x = 13-25$) as compared to the intensity of the band of pure Al (Takeuchi and Mizutani 1995) was taken as evidence for the presence of the pseudogap in these alloys. As mentioned earlier, a conclusive evidence requires probing the states above E_F . XPS valence bands of the *i*-($\text{Al}_x\text{Ga}_{1-x}$) $_{20.5}\text{Zn}_{40}\text{Mg}_{39.5}$ ($x = 0.0-0.8$) alloys (Mizutani et al. 1993) show a decrease of the XPS intensity towards E_F which is indicative of the presence of a pseudogap in this system.

It can be concluded that there is a strong spectroscopic evidence for the presence of a pseudogap in the *i*-Al-Cu-Li system and an indication of its presence in the Al-Zn-Mg and Al-Ga-Zn-Mg *i* QCs.

8.3.2 Al-Cu-Transition Metal Icosahedral Alloys

Three stable *i* alloys of high structural quality exist in the Al-Cu-TM (TM=Fe,Ru,Os) system. Electronic structure calculations were carried out for the 1/1 approximant to the *i*-Al-Cu-Fe phase by Trambly de Laissardière and Fujiwara (1994a). They predict the presence of a pseudogap with a width of ~ 0.5 eV whose center is located at ~ 0.3 eV above E_F (Fig. 6.8 in Chap. 6).

In order to establish the origin of the main features in the measured valence bands of *i*- $\text{Al}_{65}\text{Cu}_{20}\text{TM}_{15}$ alloys, the resonant-PES and PES-near-the-Cooper-minimum methods were employed (Mori et al. 1991, 1992, Stadnik and Stroink 1993, Stadnik et al. 1995a-1995c, Zhang et al. 1995). As an example, these methods are illustrated for *i*- $\text{Al}_{65}\text{Cu}_{20}\text{Os}_{15}$. For TM elements the resonance occurs at excitation energies near the *np* and *nf* thresholds. For Os one would expect the stronger $5p \rightarrow 5d$ transition at about 44.5 eV ($5p_{3/2} \rightarrow 5d$) and the weaker $4f \rightarrow 5d$ transition to take place at about 50.7 eV ($4f_{7/2} \rightarrow 5d$) (Zhang et al. 1995). The Os $5d$ -derived features should be enhanced or suppressed as $h\nu$ is swept through the $5p$ - $5d$ and $4f$ - $5d$ thresholds. It can be seen in Fig. 8.3a that, as $h\nu$ increases, the relative intensity of the peak at $BE \approx -1.5$ eV with respect to the peak at $BE \approx -3.7$ eV decreases first and reaches its minimum at $h\nu = 44.5$ eV. Then it increases slightly between $h\nu = 50$ and 60 eV. This corresponds to the stronger $5p \rightarrow 5d$ resonance (the $4f \rightarrow 5d$ resonance was too weak to be observed in the measured valence band) and indicates that the feature at $BE \approx -1.5$ eV is predominantly due to the Os $5d$ -derived states (Zhang et al. 1995).

The features in the valence bands originating from the $4d$ and/or $5d$ elements can be also identified by making use of the Cooper-minimum effect, which is the minimum in the σ_{ph} values for particular orbitals at a specific value of $h\nu$ (Stadnik et al. 1995a, 1995b, Zhang et al. 1995). Since the decrease in the σ_{ph} (Os $5d$) in the $h\nu$ range 50-200 eV is expected to be two orders of magnitude (Yeh 1993), a strong suppression of the contribution of the Os $5d$ -like states to the valence band of *i*- $\text{Al}_{65}\text{Cu}_{20}\text{Os}_{15}$ is anticipated. Figure 8.3b shows that as $h\nu$ increases from 80 eV, the relative contribution of the feature

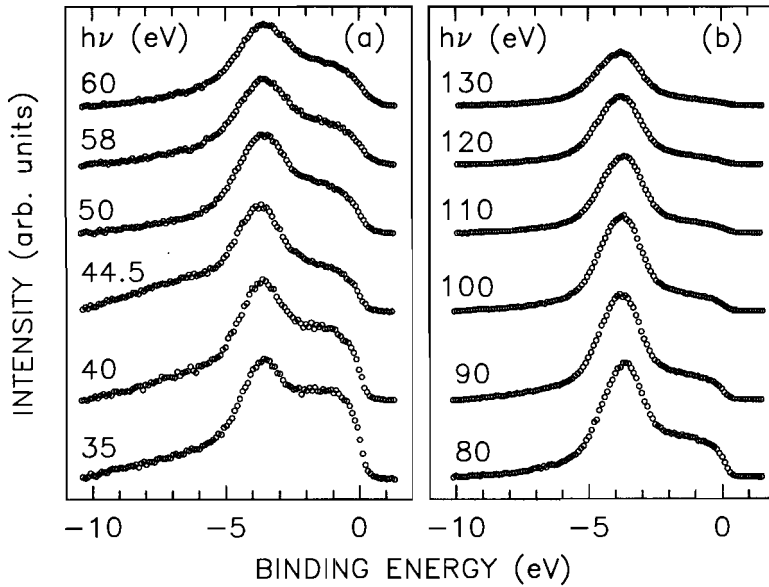


Fig. 8.3. Room-temperature valence bands of $i\text{-Al}_{65}\text{Cu}_{20}\text{Os}_{15}$ measured for different photon energies (a) around the Os $5p \rightarrow 5d$ transition and (b) around the Os $5d$ Cooper minimum. After Stadnik et al. 1995b and Zhang et al. (1995).

at $BE \approx -1.5$ eV with respect to the other feature at $BE \approx -3.7$ eV, which originates from the Cu $3d$ -derived states, decreases steadily and at $h\nu = 130$ eV is almost completely suppressed. In other words, since $\sigma_{\text{ph}}(\text{Cu } 3d)$ decreases much slower with the increase of $h\nu$ than $\sigma_{\text{ph}}(\text{Os } 5d)$, and since $\sigma_{\text{ph}}(\text{Cu } 3d)$ for $h\nu = 130$ eV is expected to be almost two orders of magnitude larger than $\sigma_{\text{ph}}(\text{Os } 5d)$ (Yeh 1993), the $h\nu = 130$ eV valence band in Fig. 8.3b must be almost entirely due to the Cu $3d$ emission.

As the bands for the $h\nu$ values around the Os $5d$ Cooper minimum exhibit much more dramatic changes in the intensity than those for the $h\nu$ values around the Os $5p \rightarrow 5d$ resonance (Fig. 8.3), the former can be used to derive the partial DOS due to Cu $3d$ -like and Os $5d$ -like states either by a direct subtraction method or by a method described below (Zhang et al. 1995). Assuming a negligible influence of the matrix-element effects, the intensity $I(h\nu, BE)$ of the valence band of $i\text{-Al}_{65}\text{Cu}_{20}\text{Os}_{15}$ can be represented by

$$I(E_B) = C(h\nu)[\sigma_{\text{Cu}}(h\nu)D_{\text{Cu}}(BE)/Z_{\text{Cu}} + \sigma_{\text{Os}}(h\nu)D_{\text{Os}}(BE)/Z_{\text{Os}}], \quad (8.1)$$

where D_i ($i = \text{Cu, Os}$) is the partial DOS of the i th element. The instrumental factor is represented by $C(h\nu)$. The partial DOS is assumed to fulfill the normalization condition,

$$\sum_i D_i \Delta BE = N_i Z_i, \quad (8.2)$$

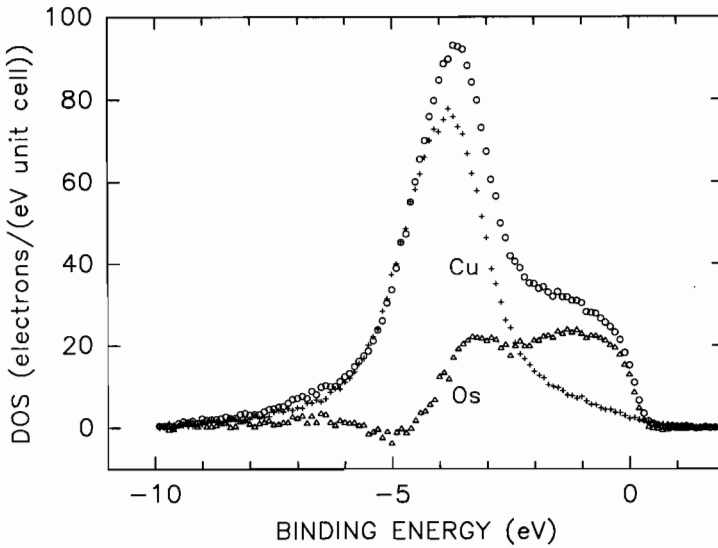


Fig. 8.4. Partial DOS of the Os 5d (triangles) and the Cu 3d (open circles) character obtained from the $h\nu = 80$ and 130 eV valence bands in Fig. 8.3b and by using the linear relation between the measured intensity and the partial DOS and σ_{ph} (Zhang et al. 1995). Their sum (full circles) represents the total DOS of the d character in $i\text{-Al}_{65}\text{Cu}_{20}\text{Os}_{15}$. After Stadnik et al. (1995b) and Zhang et al. (1995).

where N_i and Z_i are respectively the concentration and the number of d electrons of the i th element. For $i\text{-Al}_{65}\text{Cu}_{20}\text{Os}_{15}$, $N_{\text{Cu}} = 20$, $N_{\text{Os}} = 15$, and $Z_{\text{Cu}} = 10$, $Z_{\text{Os}} = 6$ (Zhang et al. 1995). By using Eq. (8.1) for two different $h\nu$ values, the partial DOS of the Cu 3d-derived and Os 5d-derived states can be obtained (Fig. 8.4).

Using Eq. (8.1), one should be able to reproduce the experimental valence bands measured for all $h\nu$ values provided that the Cu 3d and Os 5d partial DOS in Fig. 8.4 are a good measure of the true Cu 3d and Os 5d DOS in $i\text{-Al}_{65}\text{Cu}_{20}\text{Os}_{15}$. A good agreement (Fig. 8.5) between the valence bands calculated for all $h\nu$ values with the corresponding experimental valence bands confirms the reliability of the derived partial Cu 3d and Os 5d DOS (Fig. 8.4).

The results based on the resonant-PES and PES-near-the-Cooper-minimum studies of the $i\text{-Al}_{65}\text{Cu}_{20}\text{TM}_{15}$ QCs established (Mori et al. 1991, 1992, Stadnik and Stroink 1993, Stadnik et al. 1995a–1995c, Zhang et al. 1995) the origin of the two main features in the valence bands of these QCs. Also the partial d -like DOS for the QCs with $\text{TM}=\text{Ru,Os}$ were derived. For these two QCs, the experimental total and partial DOS could not be compared with theoretical DOS as these have not been calculated yet. A small measured intensity at E_F (Figs. 8.3–8.5) is indicative of a small values of $\text{DOS}(E_F)$ in these QCs. However, due to the medium energy resolution used (~ 0.4 eV) and the fact that the PES experiments were carried out at room tempera-

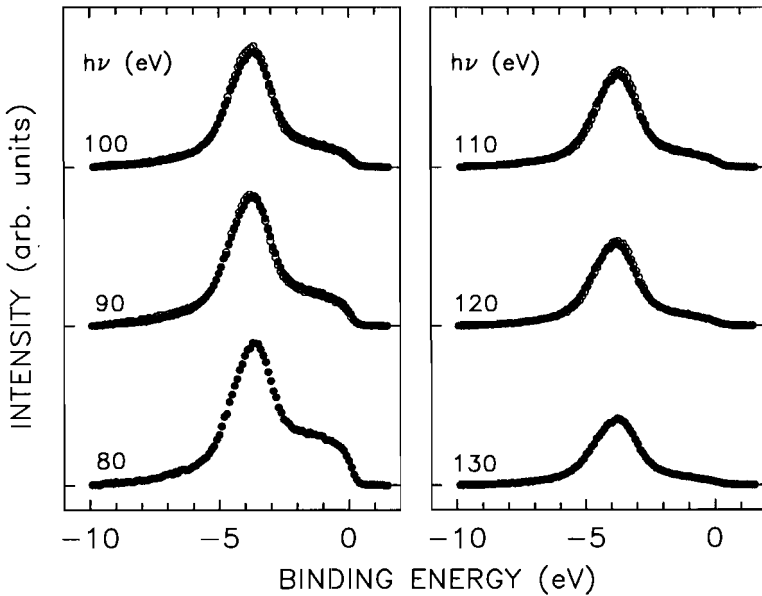


Fig. 8.5. Comparison of the valence bands generated from Eq. (8.1) using the empirical partial Cu 3*d* and Os 5*d* DOS of Fig. 8.4 (full circles) with the experimental valence bands from Fig. 8.3b (open circles). After Stadnik et al. (1995b) and Zhang et al. (1995).

ture, it was not possible to make a meaningful conclusion about the possible pseudogap as the intensity decrease toward E_F could not be separated from the Fermi edge cutoff.

The low-temperature ultraviolet photoelectron spectroscopy (UPS) He II ($h\nu = 40.8$ eV) valence bands of the *i* series Al-Cu-TM (TM=Fe,Ru,Os) have a similar two-peak structure (Fig. 8.6a). The feature at $BE \approx -4.1$ eV is mainly due to the Cu 3*d*-derived states. The resonant and the Cooper-minimum PES experiments, together with the PES experiments carried out in the constant-initial-state mode, have established (Mori et al. 1991, 1992, Stadnik and Stroink 1993, Stadnik et al. 1995a–1995c, Zhang et al. 1995) that the broad feature close to E_F is predominantly due to states of Fe 3*d*, Ru 4*d*, and Os 5*d* character, as appropriate. The positions and intensities of the Cu and Fe 3*d* features in the valence band of *i*-Al-Cu-Fe (Fig. 8.6a) agree relatively well with those obtained from the theoretical DOS (Fig. 6.8 in Chap. 6) appropriately broadened to account for the lifetime broadening effects inherent to the PES technique and the finite energy resolution of a PES experiment (Stadnik et al. 1995c).

The decrease of the spectral intensity toward E_F , which is clearly distinguishable from the Fermi-edge cutoff in the high-energy-resolution, low-temperature UPS spectra (Figs. 8.6a–8.6c), can be shown to be compatible

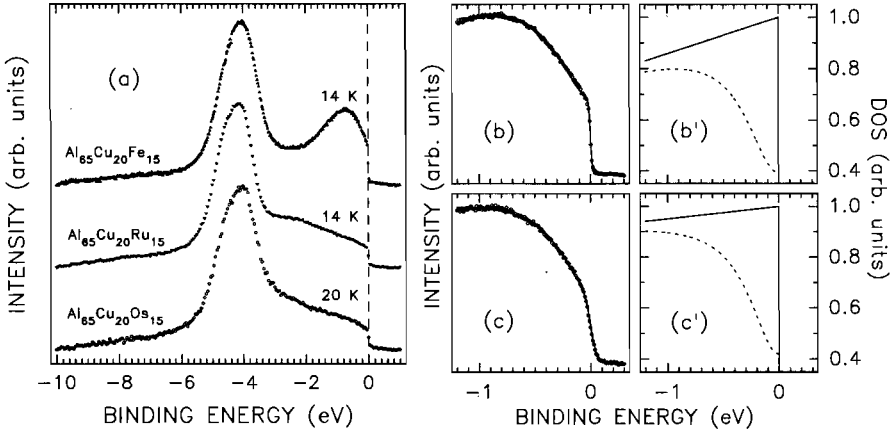


Fig. 8.6. (a) Low-temperature He II valence bands of i QCs $\text{Al}_{65}\text{Cu}_{20}\text{TM}_{15}$ (TM=Fe,Ru,Os). The energy resolution is ~ 30 meV. He II valence band regions close to E_F (open circles) of i - $\text{Al}_{65}\text{Cu}_{20}\text{Fe}_{15}$ measured at (b) 14 K and (c) 283 K with an energy resolution of 31.6(1.8) meV fitted (solid lines) with Eq. (8.1) to the corresponding model DOS in (b') and (c'). The solid lines in (b') and (c') represent the normal DOS at 0 K, and the broken lines show the Lorentzian dip which must be subtracted from the normal DOS in order to fit the valence-band regions in (b) and (c). After Stadnik et al. (1997).

with the presence of a pseudogap using the model proposed by Mori et al. (1991). As conventional alloys of QC-forming elements do not generally display a DOS minimum close to E_F , the model assumes that a simple linear extrapolation of the spectra for the BE range directly before the peak of the valence band feature close to E_F represents the DOS of an alloy without a pseudogap (the normal DOS). The presence of the pseudogap would result in an intensity dip which is assumed to be of Lorentzian shape centered at E_F , characterized by the half-width Γ_L and the dip depth C relative to the normal DOS. Thus, the observed intensity $I(E_B)$ is the convolution of the normal DOS multiplied by the pseudogap Lorentzian function and by the Fermi-Dirac function $f(E_B, T)$, and the experimental resolution Gaussian function

$$I(E_B) = \int N(ax+b) \left(1 - \frac{C\Gamma_L^2}{x^2 + \Gamma_L^2}\right) f(x, T) \exp\left[-\frac{(x - E_B)^2}{2s^2}\right] dx, \quad (8.3)$$

where N is a normalization factor, the experimental Gaussian full width at half maximum (FWHM) is related to s through $\text{FWHM} = 2\sqrt{2\ln 2}s$, and the constants a and b are determined from a linear fit of the spectra for the BE range directly before the peak of the valence band feature close to E_F . The C values of 0 and 100% correspond respectively to the normal DOS (no pseudogap) and no DOS(E_F) (full gap). This model (Figs. 8.6b' and 8.6c') fits well the near- E_F region of the valence bands of i - $\text{Al}_{65}\text{Cu}_{20}\text{Fe}_{15}$ at 14

and 283 K (Figs. 8.6b and 8.6c) for values of C and Γ_L equal to 60.5(3)%, 0.36(2) eV and 58.0(6)%, 0.33(1) eV, respectively. The width of the pseudogap is comparable to that predicted by theory. The near- E_F region of valence bands of other i -Al-Cu-TM alloys can be successfully fitted with this model (Stadnik et al. 1996, 1997, Kirihara et al. 1998), thus providing support for the existence of a pseudogap in these i alloys. It should be stressed, however, that the model does not prove the existence of the pseudogap since the PES technique probes only the occupied states.

The TS technique has the unique capability of probing the electronic states below and above E_F (Wolf 1985, Stroscio and Kaiser 1993). It is thus especially sensitive to any gap in the quasiparticle excitation spectrum at E_F which shows up directly as a characteristic feature near zero bias in the raw data conductance curves. The conductance $G = dI/dV$, where I and V are the tunnel current and the dc bias voltage [at negative (positive) sample bias, occupied (unoccupied) electron states are probed]. The G vs V dependencies are proportional to the DOS (Wolf 1985, Stroscio and Kaiser 1993). Compared to other techniques, TS has a very high energy resolution ($\sim k_B T$), which is less than 1 meV for spectra measured at liquid helium temperatures. The DOS of the i -Al_{62.5}Cu₂₅Fe_{12.5} alloy in the form of a film 3000 Å thick, which was obtained from the tunneling spectrum after the subtraction of the $E^{1/2}$ ($E = eV$) background, exhibits a pseudogap 60 meV wide which is centered at E_F (Fig. 8.7a). A similar narrow pseudogap was observed in the tunneling spectra of i -Al₆₃Cu₂₅Fe₁₂ in the ribbon form (Fig. 8.7b).

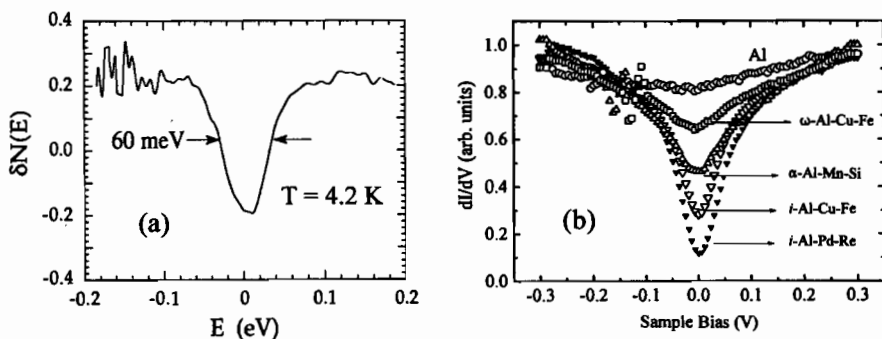


Fig. 8.7. (a) Density of states obtained from the tunneling conductance spectrum of the i -Al_{62.5}Cu₂₅Fe_{12.5} 3000 Å-thick film. After Klein et al. (1995). (b) Tunneling spectra of Al single crystal, crystalline ω -Al₇Cu₂Fe and α -Al_{72.4}Mn_{17.5}Si_{10.1} phases, and i -Al₆₃Cu₂₅Fe₁₂ and i -Al_{70.5}Pd₂₁Re_{8.5} at 4.2 K. After Davydov et al. (1996).

The observed width of a pseudogap in the TS spectra of i -Al-Cu-Fe is an order of magnitude smaller than that predicted by theory. Also its location at E_F is at variance with the predicted location at ~ 0.3 eV above E_F (Fig. 6.8 in Chap. 6). It was suggested (Klein et al. 1995, Davydov et al. 1996) that

the observed narrow pseudogap corresponds to one of the spiky structures predicted by theory rather than to a wide Hume-Rothery-like pseudogap. If this is true, then one would expect to observe at least several such structures in the tunneling spectra, which is clearly not the case (Fig. 8.7). The possible reasons for this disagreement are discussed in Sect. 8.3.7.

A crystalline alloy $\text{Al}_7\text{Cu}_2\text{Fe}$ (ω phase), which has a composition very close to that of $i\text{-Al-Cu-Fe}$ alloys but which is not an approximant to the $i\text{-Al-Cu-Fe}$ phase, is often used as a reference material in studies of the physical properties of $i\text{-Al-Cu-Fe}$ QCs. It is a metallic alloy with an electrical resistivity ρ of $22 \mu\Omega \text{ cm}$ at 4.2 K and a positive temperature coefficient of ρ (Davydov et al. 1996). Electronic structure calculations predict the presence of a pseudogap in this crystalline alloy (Belin and Mayou 1993, Trambly de Laissardière et al. 1995a, 1995b). However, the $V^{1/2}$ dependence of dI/dV observed in this alloy (Fig. 8.7b) indicates the lack of a pseudogap around E_F (Davydov et al. 1996). On the other hand, the SXE and SXA spectra were interpreted as evidence for the presence of a pseudogap in this alloy (Sadoc et al. 1993, Belin and Mayou 1993, Belin et al. 1993, Trambly de Laissardière et al. 1995a). The problem with this interpretation, which has been also used in numerous papers on the SXE and SXA studies of QCs, is related to the method of combining the SXE and SXA spectra at E_F which secures the occurrence of a pseudogap in any alloy. The measured intensity in the SXE/SXA or PES/IPES depends not only on the respective DOS but also on other factors intrinsic to the technique which are notoriously difficult to evaluate (Agrawal 1991, Fuggle and Inglesfield 1992, Kortboyer et al. 1989). This, together with a large uncertainty in the determination of the position of E_F in typical SXE/SXA measurements, makes it challenging to have a reliable combination of the SXE/SXA spectra on the same energy and intensity scale. The problem of whether there is a minimum in the DOS(E_F) in crystalline $\text{Al}_7\text{Cu}_2\text{Fe}$ remains an open question.

The Al s - and d -like unoccupied DOS in $i\text{-Al}_{65}\text{Cu}_{20}\text{Ru}_{15}$ was probed with the EELS L -edge measurements with an energy resolution of 0.12 eV (Terauchi et al. 1996). As in the UPS spectrum of this alloy (Fig. 8.6a), a clear Fermi edge was observed (Fig. 8.8) which proves that this alloy, in spite of its very high value of ρ , is metallic. As compared to the Al L -edge spectrum of Al metal measured with a resolution of 0.2 eV, the L_3 edge is shifted by 0.2 eV to 73.1 eV (Fig. 8.8). The key features of the Al L -edge spectrum of $i\text{-Al}_{65}\text{Cu}_{20}\text{Ru}_{15}$ is a small rise of intensity at the L_3 edge as compared to that of Al metal and "scooping out" of the DOS near the edge onset. This indicates the occurrence of the pseudogap of the estimated half width at half maximum of ~ 0.9 eV in the Al s and d states at E_F (Terauchi 1996, 1998a).

In summary, spectroscopic data reviewed above (Davydov et al. 1996, Kirihara et al. 1998, Klein et al. 1995, Mori et al. 1991, Stadnik et al. 1996, 1997, Terauchi 1996, 1998a) are compatible with the presence of the pseudogap in the DOS around E_F in the $i\text{-Al-Cu-TM}$ (TM=Fe,Ru,Os) alloys.

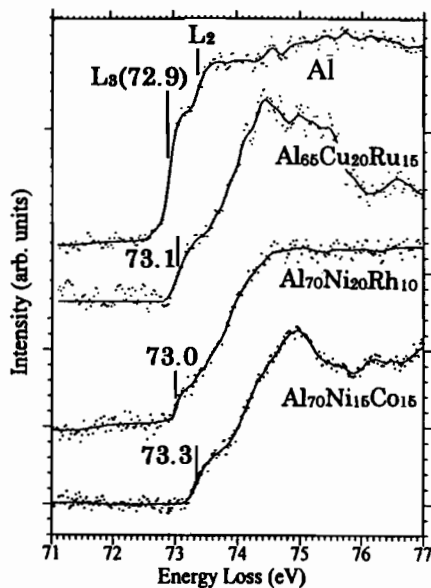


Fig. 8.8. EELS Al L -edge spectra of Al, i QC $Al_{65}Cu_{20}Ru_{15}$, and d QCs $Al_{70}Ni_{20}Rh_{10}$ and $Al_{70}Ni_{15}Co_{15}$. After Terauchi et al. (1998a).

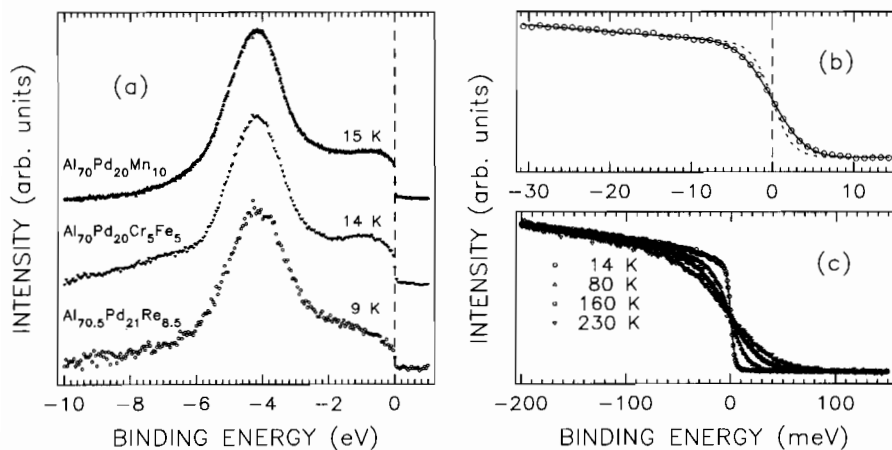


Fig. 8.9. (a) Low-temperature He II valence bands of Al-Pd-based i QCs. The energy resolution is ~ 30 meV. (b) Near- E_F He I valence band of $i-Al_{70}Pd_{20}Mn_{10}$ at 14 K. The solid line is the fit to a linearly decreasing intensity multiplied by the Fermi-Dirac function at 14 K (broken curve) and convoluted with a Gaussian whose FWHM = $5.8(2)$ meV. The step between the data points is 1 meV. (c) Near- E_F He I valence band of $i-Al_{70}Pd_{20}Mn_{10}$ measured at different temperatures. The solid lines are the fits as described in (b). Note the different BE scales in (b) and (c). After Stadnik et al. (1996, 1997) and Stadnik and Purdie (1997).

8.3.3 Al-Pd-Mn Icosahedral Alloys

The electronic structure calculations carried out for approximants to the i phase (Krajčí et al. 1995) predict a structure-induced minimum slightly above E_F in the DOS (Fig. 7.14 in Chap. 7). This minimum is strongly pronounced in the Al band and rather weakly formed in the Pd and Mn bands.

The low-temperature UPS He II valence band of i -Al₇₀Pd₂₀Mn₁₀ (Fig. 8.9a) has a two-peak structure. As is shown below, the feature at $BE \approx -4.2$ eV is mainly due to the Pd 4d-like states, and the broad feature close to E_F is predominantly due to the states of the Mn 3d character. A clear presence of the Fermi edge in the near- E_F UPS He I ($h\nu = 21.2$ eV) valence band (Fig. 8.9b) and its temperature evolution following the Fermi-Dirac function (Fig. 8.9c) show that i -Al₇₀Pd₂₀Mn₁₀, in spite of its large ρ , is metallic.

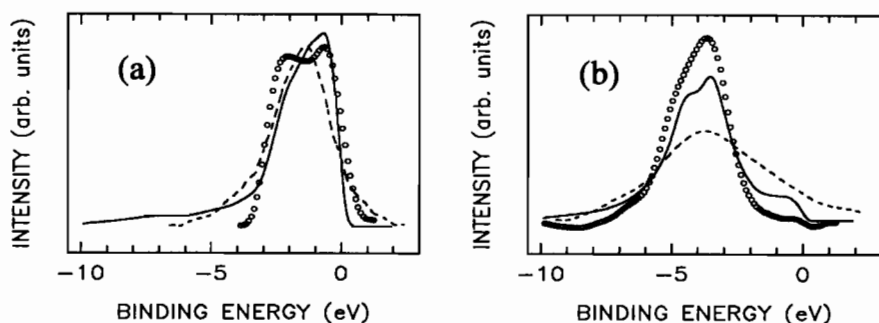


Fig. 8.10. Comparison of the partial DOS of the Mn 3d (a) and Pd 4d (b) character in i -Al-Pd-Mn obtained from the PES spectra (open circles, Zhang et al. 1994) and from the SXE measurements (dashed line, Belin et al. 1994a) with the corresponding broadened theoretical partial DOS (solid line, Krajčí et al. 1995). After Zhang and Stadnik (1995).

The occupied partial d -like and total DOS predicted by theory (Krajčí et al. 1995) for i -Al-Pd-Mn compare well with those determined from the room-temperature PES measurements on i -Al₇₀Pd₂₀Mn₁₀ (Zhang et al. 1994, Zhang and Stadnik 1995). This is illustrated in Fig. 8.10 where the partial DOS of the Mn-3d and Pd-4d character, which were derived from the PES spectra measured with an energy resolution of ~ 0.4 eV for $h\nu$ values close to the Pd 4d Cooper minimum (Zhang et al. 1994), are compared with the corresponding calculated DOS of the 8/5 approximant to the i phase (Fig. 7.14 in Chap. 7) which were appropriately broadened (Zhang and Stadnik 1995) to account for the lifetime broadening effects inherent to the PES technique and for the finite resolution of a PES experiment. There is a notable agreement with respect to the overall structure of the partial Mn 3d and Pd 4d DOS. This structure is not present in the SXE spectra (Fig. 8.10) due to severe

lifetime broadening effects inherent to the SXE transitions probing the Mn and Pd d states (Zhang and Stadnik 1995).

In order to compare the theoretical total DOS calculated for the 8/5 approximant to the i phase (Fig. 7.14 in Chap. 7) with the valence band of i -Al₇₀Pd₂₀Mn₁₀ measured at a given $h\nu$, the theoretical Al, Pd, and Mn partial DOS have to be first multiplied by the corresponding σ_{ph} at that $h\nu$. The sum of the products of the theoretical partial DOS and the corresponding σ_{ph} , which was broadened in the same way as described above, compares well with the experimental valence band measured at $h\nu = 100$ eV (Fig. 8.11). It is thus concluded that the theoretical occupied DOS (Krajčí et al. 1995) agrees well with the measured PES spectra (Stadnik et al. 1996, 1997, Zhang et al. 1994, Zhang and Stadnik 1995).

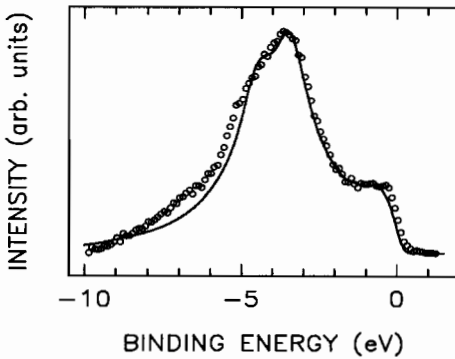


Fig. 8.11. Comparison of the valence band of i -Al₇₀Pd₂₀Mn₁₀ measured at $h\nu = 100$ eV (open circles, Zhang et al. 1994) with the broadened theoretical DOS for the 8/5 approximant to the i phase (solid line, Krajčí et al. 1995). After Zhang and Stadnik (1995).

The existence of a pseudogap in the DOS at E_{F} cannot be determined unambiguously from the PES spectra measured at room temperature with a medium resolution of 0.4 eV (Fig. 8.11) in which the decrease of the spectral intensity due to the possible presence of the pseudogap cannot be distinguished from the Fermi cutoff. The near- E_{F} region of the low-temperature UPS spectrum of i -Al₇₀Pd₂₀Mn₁₀ (Fig. 8.9a) can be fitted well to Eq. (8.3) and this can be interpreted as being compatible with the presence of the pseudogap at E_{F} with $\Gamma_{\text{L}} = 0.22(2)$ eV (Stadnik et al. 1996, 1997).

The lack of the Fermi edge in the angle-resolved, high-energy-resolution (50 meV), room-temperature PES valence band of a single-grain i alloy Al₇₀Pd_{21.5}Mn_{8.5} was interpreted (Wu et al. 1995) as direct evidence of a pseudogap in the DOS near E_{F} . However, this is in contradiction to the presence of the Fermi edge in the high-energy-resolution low-temperature spectra of both polyquasicrystalline (Fig. 8.9) and single-grain (Purdie et al. 1998) i -Al-Pd-Mn alloys.

An unambiguous experimental evidence for the presence of the pseudogap was provided by a PES experiment with an energy resolution of 70 meV (Neuhold et al. 1998) on a single grain i -Al_{70.5}Pd₂₁Mn_{8.5} at 570 K. In this

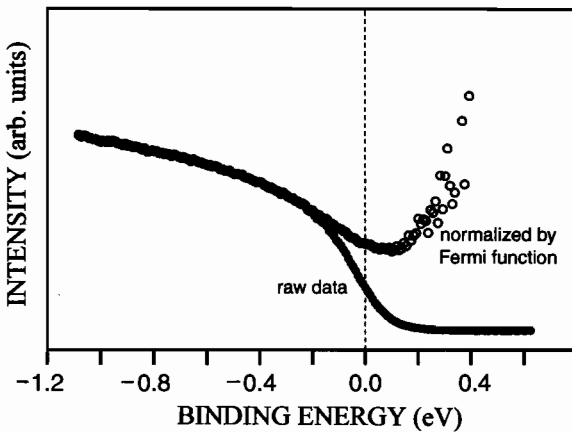


Fig. 8.12. Valence band of $i\text{-Al}_{70.5}\text{Pd}_{21}\text{Mn}_{8.5}$ at 570 K measured at $h\nu = 32.3$ eV (full circles) and the reconstructed spectral function (open circles) near E_F . After Neuhold et al. (1998).

experiment, the states both below and above E_F were probed. The PES technique can probe the states also above E_F if they are populated. According to Fermi-Dirac statistics, in metallic systems these states become populated at nonzero temperatures (Fig. 8.9c). At a temperature of 570 K, a region of several hundred meV above E_F becomes accessible (Fig. 8.12). A spectral function, which is proportional to the DOS, can be reconstructed from the 570 K valence band (Neuhold et al. 1998). It clearly shows a minimum of DOS located at 90 meV above E_F (Fig. 8.12). For BE 's higher than ~ 0.3 eV ($6.1k_B T$), a considerable scatter of the reconstructed spectral function, which is due to the small probability that the states are populated, prevents a meaningful evaluation of the DOS. It should be noted (Neuhold et al. 1998) that accessing states slightly above E_F through the method described above is superior to IPES or SXA because of the much higher energy resolution.

The optical conductivity studies in the energy range 0.001–12 eV of $i\text{-Al}_{70}\text{Pd}_{21}\text{Mn}_9$ showed the presence of a large absorption in the conductivity spectrum at ~ 1.2 eV (Bianchi et al. 1993, 1998). This absorption was interpreted to result from excitations across a pseudogap in the DOS.

The PES core-line asymmetry, whose measure is the asymmetry parameter α in the Doniach–Šunjić formula describing the shape of the PES core-level lines (Cardona and Ley 1978, Mehlhorn 1982), is proportional to the local $\text{DOS}(E_F)$: the larger α indicates the larger local $\text{DOS}(E_F)$, (Mehlhorn 1982). An increase of α determined from the fits of the Al 2p lines measured with the resolution of 180 meV for different values of $h\nu$ (Fig. 8.13a), and thus different electron kinetic energies, E_{kin} , as a function of E_{kin} was observed for the single-grain $i\text{-Al}_{70.5}\text{Pd}_{21}\text{Mn}_{8.5}$ alloy (Fig. 8.13b). No such increase could be observed for a fcc Al metal (Fig. 8.13b). The value of E_{kin} is a measure of

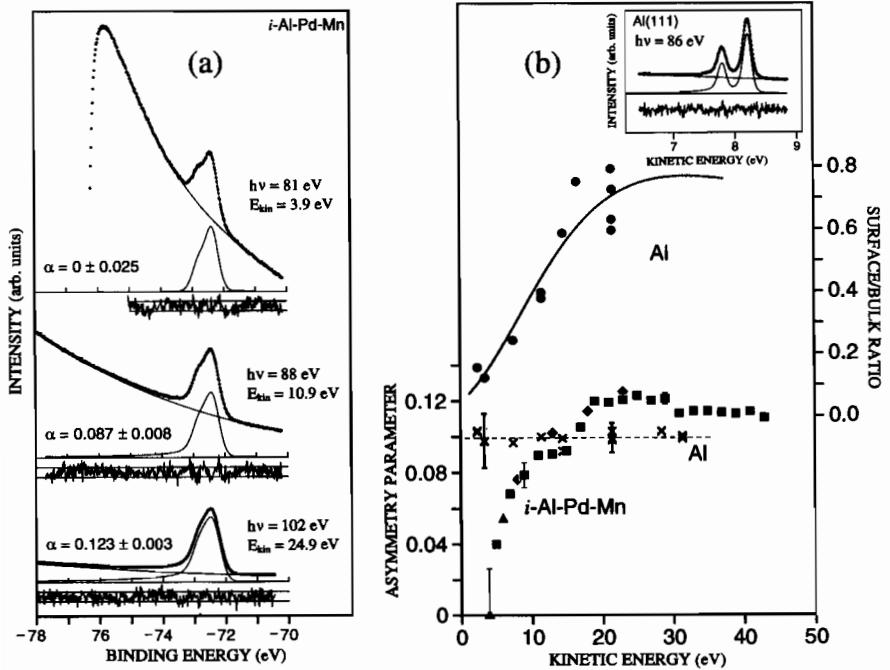


Fig. 8.13. (a) Al 2p core-level spectra of *i*-Al_{70.5}Pd₂₁Mn_{8.5} measured at different photon energies. The solid lines for each spectrum represent the fits of the background and the Doniach–Šunjić doublet. The residuals to the fits are also shown with the upper and lower bounds at $\pm\sqrt{N}$ (N is the number of counts) determined from the Poisson statistics. (b) Lower part: Asymmetry parameter of the Al 2p core-level lines of *i*-Al_{70.5}Pd₂₁Mn_{8.5} (full symbols) and fcc Al (crosses) as a function of the electron kinetic energy. Upper part: Surface to bulk intensity ratio determined from the Al 2p core-level lines of a single-crystal Al(100). The solid line is calculated from theory. Inset: Al 2p core-level lines of a single-crystal Al(111). After Neuhold et al. (1998).

the sampling depth of a PES experiment by virtue of inelastic electron scattering in a sample: the larger E_{kin} , the smaller the sampling depth, i.e., the more surface contribution to the measured PES intensity (Cardona and Ley 1978, Mehlhorn 1982, Hüfner 1996). The sampling depth dependence upon E_{kin} was measured through the relative intensity of the surface to bulk Al 2p core-level lines (Fig. 8.13b) for a single crystal Al(100) for which surface and bulk signals can be separated. A similar dependence upon E_{kin} of α and of the surface to bulk ratio (Fig. 8.13b) was interpreted as indicating that α for atoms near the surface of *i*-Al_{70.5}Pd₂₁Mn_{8.5} is larger than α for those in the bulk. Since α is proportional to $DOS(E_F)$, this observation was claimed to provide evidence for the higher $DOS(E_F)$ at the surface than in the bulk in *i*-Al_{70.5}Pd₂₁Mn_{8.5} (Neuhold et al. 1998).

This interpretation is valid provided that the values of α derived from the fits is meaningful. As it can be seen from the Al $2p$ PES spectrum of Al(111) (inset in Fig. 8.13b), the Al $2p_{1/2}$ and $2p_{3/2}$ components are clearly separated and consequently the value of α can be precisely determined. However, this separation is absent in the corresponding spectra of the i -Al-Pd-Mn alloy (Fig. 8.13a). This is due the multiplicity of Al sites, and thus the multiplicity of the local chemical surroundings (see Sect. 8.4) around Al atoms in a quasicrystalline structure, as demonstrated experimentally by various local probes (Stadnik 1996). One would thus expect that the measured Al $2p$ spectrum results from a superposition of the Doniach–Šunjić lines corresponding to these sites, which naturally leads to the distribution of the parameters characterizing a Doniach–Šunjić profile. It is therefore not obvious whether fitting the measured Al $2p$ line with one Doniach–Šunjić line profile provides a meaningful average value of α corresponding to a given E_{kin} . Since different core levels should have the same α (Hüfner 1996), it would be important to carry out similar measurements for other TM core-level lines in order to establish the validity of the observation that α is smaller at the surface than in the bulk of i alloys.

The availability of high-quality i -Al-Pd-Mn samples made it possible to observe the de Haas–van Alphen effect (Shoenberg 1984) in a single grain i -Al₇₀Pd_{21.5}Mn_{8.5} (Haanappel et al. 1996). Two well-defined frequencies were observed for the magnetic field along the fivefold direction and two other frequencies were detected for the field parallel to the two fold direction. These observations are indicative of the reality of the Fermi surface in QCs, which has probably a very complex shape (Fujiwara 1998). The first attempts to calculate the shape of the Fermi surface in QCs indicate that it has a complex shape. It would be an experimental challenge to determine its size and shape using the the de Haas–van Alphen effect and other spectroscopic techniques.

The spectroscopic results presented above confirm the presence of the predicted minimum of the DOS slightly above E_F and are in good agreement with the predicted overall structure of the occupied DOS in i -Al-Pd-Mn (Krajčič et al. 1995).

8.3.4 Al-Pd-Re Icosahedral Alloys

Among all QCs, the i -Al-Pd-Re alloys distinguish themselves in exhibiting the highest ρ and the extreme sensitivity of their physical properties to minute changes in their composition (see Chap. 5). It was even suggested that the i -Al-Pd-Re alloys are insulators at low temperatures (Pierce et al. 1993a, 1994), but this claim was recently disputed (Ahlgren et al. 1997, Bianchi et al. 1997). The recent electronic structure calculations (Krajčič and Hafner 1998) predict that a minute change of stoichiometry of the 1/1 approximant to the i -Al-Pd-Re phase may change it from being a metal with a pseudogap to a narrow-gap semiconductor with a real gap of the width ~ 0.15 eV located

just below E_F . For higher-order approximants, no real gaps, but a series of pseudogaps around E_F is predicted (Fig. 7.16 in Chap. 7).

The low-temperature UPS He II valence band of $i\text{-Al}_{70.5}\text{Pd}_{21}\text{Re}_{8.5}$ (see Fig. 8.9a) exhibits a feature at $BE \approx -4.1$ eV mainly due to the Pd 4d-like states and a very broad feature close to E_F predominantly due to the states of the Re 5d character (Stadnik et al. 1996, 1997). The positions and intensities of these features are in good agreement with the calculated DOS (Fig. 7.16 in Chap. 7). There is a noticeable smaller spectral intensity at E_F in the valence band of $i\text{-Al}_{70.5}\text{Pd}_{21}\text{Re}_{8.5}$ in comparison to that of other Al-Pd-based i alloys (Fig. 8.9a), which is indicative of a smaller $\text{DOS}(E_F)$ in this alloy than in other i alloys. The near- E_F region of the valence band of $i\text{-Al}_{70.5}\text{Pd}_{21}\text{Re}_{8.5}$ can be well fitted to Eq. (8.3), which can be interpreted as indicative of the presence of a pseudogap at E_F of the FWHM ($2\Gamma_L$) of $\sim 200\text{--}400$ meV (Purdie and Stadnik 1997, Stadnik et al. 1996, 1997). This width is several times wider than that of ~ 60 meV found in the TS spectrum (Fig. 8.7b).

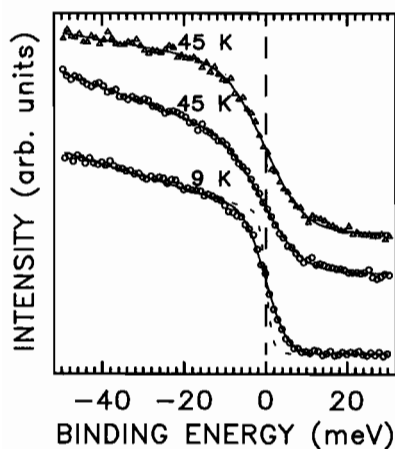


Fig. 8.14. Near- E_F He I valence bands of $i\text{-Al}_{70.5}\text{Pd}_{21}\text{Re}_{8.5}$ (circles) and Ag (triangles) evaporated on it. The solid lines are the fits to a linearly decreasing intensity multiplied by the Fermi-Dirac function at 45 and 9 K (broken curve) and convoluted with a Gaussian whose FWHM is respectively 6.0(5) and 9.2(3) meV for the spectra measured at 45 and 9 K. After Stadnik et al. (1998).

The optical conductivity studies carried out in the energy range 0.001–12 eV on two i samples, $\text{Al}_{70}\text{Pd}_{20}\text{Re}_{10}$ and $\text{Al}_{70}\text{Pd}_{21.4}\text{Re}_{8.6}$, showed a large absorption in the conductivity spectra at ~ 2.6 eV (Bianchi et al. 1997). This absorption was interpreted as resulting from excitations across a pseudogap in the DOS.

The low-temperature near- E_F UPS He I spectra of $i\text{-Al}_{70.5}\text{Pd}_{21}\text{Re}_{8.5}$ measured with the highest energy resolution presently available (Fig. 8.14) clearly show the presence of a Fermi edge. This can be seen by comparing a near- E_F spectrum at 45 K of $i\text{-Al}_{70.5}\text{Pd}_{21}\text{Re}_{8.5}$ with that of Ag evaporated onto the alloy. Additional evidence comes from the perfect fits of the spectra of this alloy measured at 45 and 9 K (Fig. 8.14). This constitutes a direct proof that the $i\text{-Al}_{70.5}\text{Pd}_{21}\text{Re}_{8.5}$ alloy, in spite of its very high ρ , is metallic, supporting

the same conclusion based on low-temperature ρ measurements by Ahlgren et al. (1997) and Bianchi et al. (1997). The finite value of G for the zero sample bias (Fig. 8.7b) indicates a finite DOS(E_F), and thus a metallic character of the i -Al-Pd-Re QC.

The above analysis of the spectroscopic data on the occupied and unoccupied DOS provides conclusive evidence for the presence of the theoretically predicted pseudogap in the Al-Cu-Li and Al-Pd-Mn i alloys. For other investigated i QCs, the data are compatible with the presence of the pseudogap. A generally good agreement between the calculated and measured DOS is observed, which indicates that the essential ingredients of the electronic structure of QCs can be obtained from the calculations carried out for their approximants.

8.3.5 Al-Co-Cu Decagonal Alloys

The low-temperature He II valence band of d -Al₆₅Co₁₅Cu₂₀ exhibits two features (Fig. 8.15). As shown earlier with the resonance PES technique (Stadnik et al. 1995d), the feature close to E_F is predominantly due to states of Co 3d character and the feature at $BE \approx -4.2$ eV is mainly due to the Cu 3d-derived states. The resonance PES data enabled the derivation of the partial DOS of the Co and Cu 3d character and a significant discrepancy between the theoretical (Trambly de Laissardière and Fujiwara 1994b, 1994c) and experimental Co 3d DOS was found (Stadnik et al. 1995d). This is illustrated in Fig. 8.16 where a much larger experimental intensity at E_F due to the Co 3d states as compared to that expected from the presence of a pseudogap can be seen. This was taken as evidence for the absence of a pseudogap in the d -Al₆₅Co₁₅Cu₂₀ alloy (Stadnik et al. 1995d).

The electronic structure calculations (Krajčí et al. 1997a) based upon several variants of the original Burkov model for the atomic structure of d -Al-Co-Cu show the best agreement with the PES data from Fig. 8.16 (Fig. 7.15 in Chap. 7) for the variant B2Cu. There is no pseudogap in the DOS(E_F) for this variant of the atomic structure of d -Al-Co-Cu.

The successful fit of the near- E_F UPS He II valence band of the d -Al₆₅Co₁₅Cu₂₀ alloy with Eq. (8.3) led to the conclusion (Stadnik et al. 1997) of the presence of the pseudogap in this alloy, which is in contradiction to the conclusion based on the analysis of the PES data (Stadnik et al. 1995d, Krajčí et al. 1997a). There is some arbitrariness in the model expressed by Eq. (8.3) regarding the choice of the BE range for which the data are fitted to a line $aBE + b$ representing a normal DOS. This range was chosen much farther away from E_F for d alloys (leading to the normal DOS with a positive slope) than for i alloys (Stadnik et al. 1997). In view of the DOS calculated for the structural variant B2Cu [Fig. 8 in Krajčí et al. (1997a)], the assumption of the normal DOS with the positive slope may be unwarranted; the choice of the BE range closer to E_F would lead to no pseudogap in the fit of the near- E_F UPS He II valence band of d -Al₆₅Co₁₅Cu₂₀. Clearly,

further spectroscopic data, especially those probing the unoccupied DOS, are needed to unambiguously determine the presence or lack of the pseudogap in the d -Al-Co-Cu system.

8.3.6 Al-Ni-Co and Al-Ni-Rh Decagonal Alloys

No electronic structure calculations have been carried out yet for the two d systems, Al-Ni-Co and Al-Ni-Rh, which would allow a comparison to be made with the spectroscopic data on the occupied and unoccupied DOS. The valence band of d -Al₇₀Co₁₅Ni₁₅ (Depero and Parmigiani 1993, Stadnik et al. 1995d, 1997) consists of a broad feature (Fig. 8.15) resulting from the overlap of the Co and Ni 3d states (Stadnik et al. 1995d).

The Al K α XPS valence band of d -Al₇₀Co₁₅Ni₁₅, which was measured at room temperature with an energy resolution of 0.3 eV, was interpreted as showing no presence of the pseudogap (Depero and Parmigiani 1993); no justification of this interpretation was given. The presence of significant intensity at the E_F due to Co and Ni 3d-like states in the PES bands, which were measured at room temperature for different values of $h\nu$ and with an energy resolution of ~ 0.4 eV, was taken as an indication for the lack of a pseudogap (Stadnik et al. 1995d). On the other hand, the successful fit of the near- E_F UPS He II valence band of d -Al₇₀Co₁₅Ni₁₅ with Eq. (8.3) led to the conclusion (Stadnik et al. 1997) that there is a pseudogap of the width $2\Gamma_L \approx 2.2$ eV in this alloy. As indicated above, the assumption of the normal DOS with the positive slope, which leads to the pseudogap, may be not justified for d alloys. However, a combination of the PES and IPES

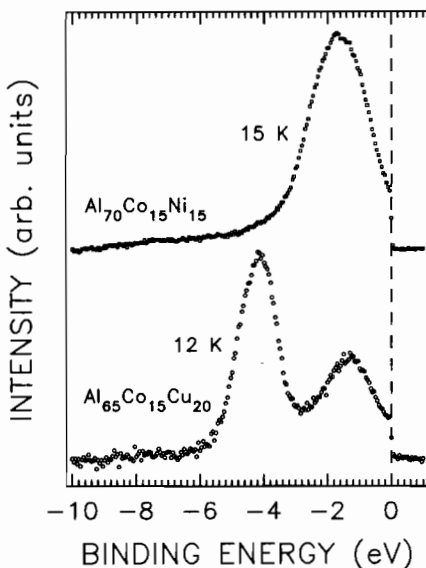


Fig. 8.15. Low-temperature He II valence bands of d QCs Al₆₅Co₁₅Cu₂₀ and Al₇₀Co₁₅Ni₁₅. The energy resolution is ~ 30 meV. After Stadnik et al. (1998).

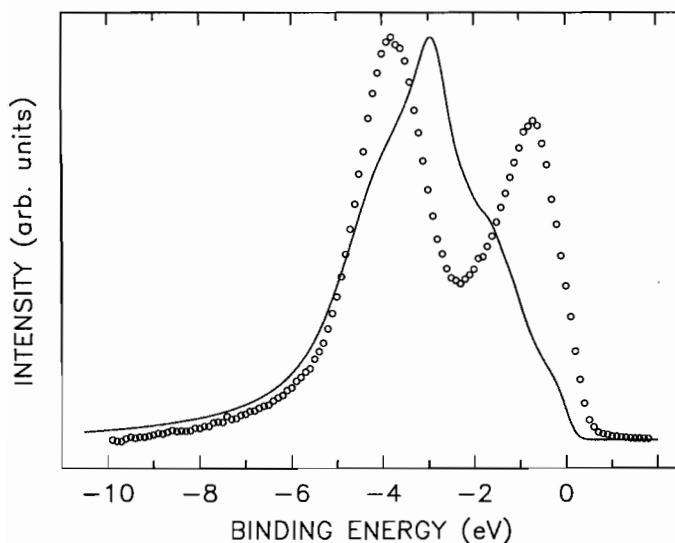


Fig. 8.16. Comparison between the room-temperature valence band of $d\text{-Al}_{65}\text{Co}_{15}\text{Cu}_{20}$ measured at $h\nu = 100$ eV with an energy resolution of ~ 0.4 eV (open circles) and the appropriately broadened theoretical DOS (solid line) calculated by Trambly de Laissardière and Fujiwara (1994b, 1994c). After Stadnik et al. (1995d).

techniques shows the presence of the pseudogap of the width of ~ 1.7 eV in the total DOS of $d\text{-Al}_{72}\text{Co}_{16}\text{Ni}_{12}$ (Fig. 8.17).

The presence of a step structure above a Fermi edge in the EELS Al L -edge spectrum of $d\text{-Al}_{65}\text{Co}_{15}\text{Ni}_{15}$ (Fig. 8.8), which was measured with an energy resolution of 0.15 eV, was interpreted as evidence for the presence of a pseudogap in the DOS of the Al s - and d -like states (Terauchi et al. 1998a, 1998b). A similar conclusion was reached by Soda et al. (1998a) based on the Al $L_{2,3}$ SXE and SXA spectra of $d\text{-Al}_{72}\text{Co}_{16}\text{Ni}_{12}$ (Fig. 8.18).

The optical conductivity studies in the energy range 0.001–12 eV of a single grain $d\text{-Al}_{71}\text{Co}_{16}\text{Ni}_{13}$ (Bianchi et al. 1998) revealed absorptions for the periodic direction at ~ 1 eV, and for a direction in the quasiperiodic plane at ~ 2 eV. These absorptions were interpreted as evidence for the electronic excitations across a pseudogap.

The EELS Al L -edge spectrum of $d\text{-Al}_{70}\text{Ni}_{20}\text{Rh}_{10}$ (Fig. 8.8), which was measured with an energy resolution of 0.12 eV (Terauchi et al. 1998c), exhibits a step structure above the Fermi edge. This was interpreted as evidence for the presence of a pseudogap in the DOS of the Al s - and d -like states (Terauchi et al. 1998c). No other spectroscopic data are available for this alloy system.

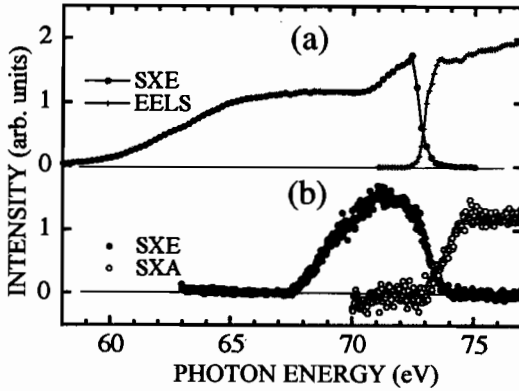


Fig. 8.17. (a) IPES spectrum of Au. (b) PES and IPES spectra of $d\text{-Al}_{72}\text{Co}_{16}\text{Ni}_{12}$. The solid lines are the smoothed experimental data. After Soda et al. (1998a).

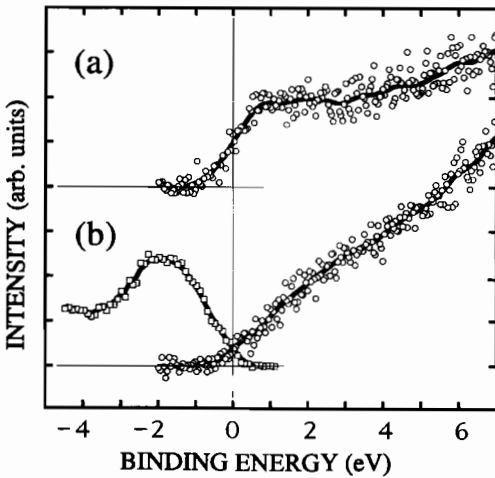


Fig. 8.18. Comparison between (a) SXE Al $L_{2,3}$ and EELS Al L-edge spectra of Al and (b) Al $L_{2,3}$ SXE and SXA spectra of $d\text{-Al}_{72}\text{Co}_{16}\text{Ni}_{12}$. After Soda et al. (1998b).

Thus it can be concluded that there is strong spectroscopic evidence for the existence of the pseudogap in the DOS in the $d\text{-Al-Co-Ni}$ system and some indication for its existence in the $d\text{-Al-Ni-Rh}$ system.

8.3.7 Fine Structure of the Density of States

In order to assess the possible existence of the predicted DOS spikiness, a meaningful comparison between the measured DOS spectra and the calculated DOS has to be made. This involves modifying the theoretical DOS to account for the finite energy resolution of an experiment, the lifetime broadening effects inherent to a given spectroscopic technique used to measure the DOS, and the sample temperature (Stadnik et al. 1995a). The instrumental broadening is usually represented by a Gaussian with the FWHM, Γ_G , equal to the energy resolution of an experiment. The lifetime broadening effects are usually described by a Lorentzian whose FWHM is in the form $\Gamma_L^0 BE^2$,

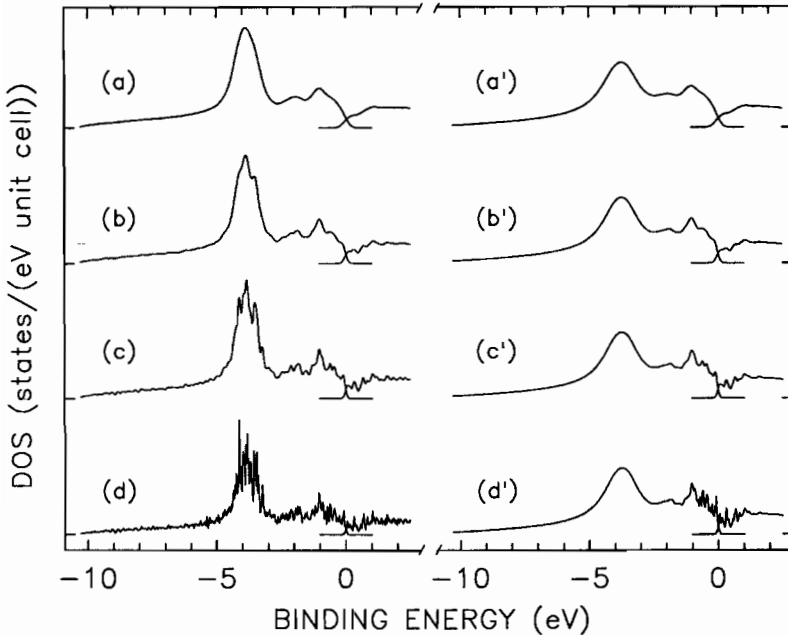


Fig. 8.19. Left panel: DOS from Fig. 6.8 in Chap. 6 convoluted with a Gaussian with Γ_G equal to (a) 0.4 eV, (b) 0.2 eV, (c) 0.1 eV, and (d) 0.025 eV, and multiplied by the Fermi-Dirac function at room temperature. Right panel: DOS from Fig. 6.8 in Chap. 6 convoluted with a Lorentzian with $\Gamma_L^0 = 0.05 \text{ eV}^{-1}$ and a Gaussian with Γ_G equal to (a') 0.4 eV, (b') 0.2 eV, (c') 0.1 eV, and (d') 0.025 eV, and multiplied by the Fermi-Dirac function at room temperature. The separation between the two neighboring ticks on the ordinate scale corresponds to 380 states/(eV unit cell) and the DOS values in plot (d) were divided by the factor 1.47. After Stadnik et al. (1995a).

where the Γ_L^0 parameter fixes the scale of broadening. Assuming a hypothetical case of a PES experiment on a QC at room temperature with no lifetime broadening effects (left panel in Fig. 8.19), an energy resolution better than $\sim 0.2 \text{ eV}$ would be required to detect the spikes. The inclusion of the lifetime broadening effects (right panel in Fig. 8.19) smears the sharp features of the DOS in proportion to the square of their distance from E_F . It is clear that the possible DOS spikiness can be observed in a QC sample at room temperature with the spectroscopic techniques with an energy resolution better than $\sim 100 \text{ meV}$, and only in the vicinity of E_F .

In view of the analysis presented above, it is not surprising that no spikiness was observed in PES/IPES experiments carried out with a resolution $\geq 0.1 \text{ eV}$ (Matsubara et al. 1991, Mori et al. 1992, 1993, Stadnik and Stroink 1993, Stadnik et al. 1995, Takeuchi and Mizutani 1995, Zhang and Stadnik 1995, Zhang et al. 1994, 1995). The claim (Belin et al. 1994b) of experimental evidence of the presence of DOS spikiness in the Al p -like DOS in

$i\text{-Al}_{62.5}\text{Cu}_{26.5}\text{Fe}_{11}$, which was based on the observation of a low-intensity structureless SXA Al p conduction band, is unfounded in view of the poor energy resolution and severe lifetime broadening effects inherent to the SXA technique. However, no DOS spikiness could be observed also in high-energy-resolution PES spectra of QCs at room temperature. Wu et al. (1995) observed no fine structure in the near- E_F valence band of a single grain $i\text{-Al}_{70}\text{Pd}_{21.5}\text{Mn}_{8.5}$ measured at $h\nu = 13$ eV with an energy resolution of 50 meV. No DOS spikiness was observed in the UPS He II near- E_F valence band of $i\text{-Al}_{65}\text{Cu}_{20}\text{Fe}_{15}$ at 283 K measured with an energy resolution of 32 meV (Fig. 8.6c).

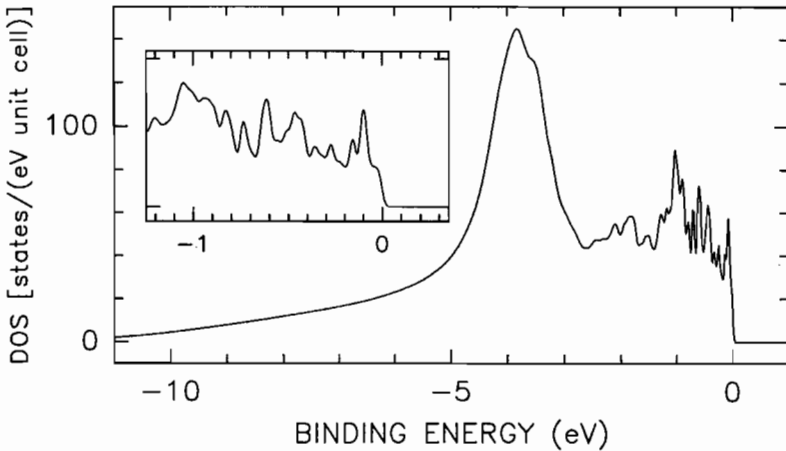


Fig. 8.20. Occupied part of the DOS from Fig. 6.8 in Chap. 6 multiplied by the Fermi-Dirac function at 14 K and convoluted with a Lorentzian with $\Gamma_L^0 = 0.02$ eV $^{-1}$ and a Gaussian with $\Gamma_G = 31.6$ meV. The values of temperature and Γ_G correspond to the experimental spectrum in Figs. 8.6(a) and 8.6(b). The inset shows the DOS in the vicinity of E_F . The two ticks on the ordinate axis of the inset correspond, respectively, to 0 and 100 states/(eV unit cell). After Stadnik et al. (1995a).

Figure 8.20 shows the expected low-temperature He II valence band of $i\text{-Al-Cu-Fe}$. It was calculated based on the DOS from Fig. 6.8 in Chap. 6 which was broadened using the values of temperature and Γ_G corresponding to the experimental spectra of $i\text{-Al}_{65}\text{Cu}_{20}\text{Fe}_{15}$ in Figs. 8.6a and 8.6b. The Γ_L^0 value used is a typical value employed for metallic systems (Stadnik et al. 1997). It is clear that the predicted DOS spikiness should be observed for BE 's up to a few eV below E_F in low-temperature UPS valence bands of QCs measured with the high energy resolution of a few tens of meV. Obviously, the DOS spikes should be observed even more readily for the ultrahigh energy resolution (< 10 meV). However, no spikes could be found in the low-temperature valence bands of i alloys measured with high (Figs. 8.6

and 8.9a) or ultrahigh (Figs. 8.9b, 8.9c, and 8.14) energy resolution (Stadnik et al. 1996, 1997, Kirihara et al. 1998, Neuhold et al. 1998). Such spikes were also not detected in the high- and ultrahigh-energy-resolution UPS valence bands of *d* QCs (Stadnik et al. 1997).

TS experiments, which have an energy resolution perhaps better than 1 meV, showed no evidence of spiky features in the occupied and unoccupied DOS for energies up to 300 meV around E_F (Klein et al. 1995, Davydov et al. 1996). Contradictory conclusions concerning DOS spikiness were reported based on the indirect studies of the DOS with a NMR technique. In a NMR pressure study of *i*-Al₆₅Cu₂₀Ru₁₅, DOS fine structure was expected to be probed on the 10 meV energy scale through the pressure dependence of the Knight shift K_s and the spin-lattice relaxation rate R_1 (Shastri et al. 1995). Since no such dependence of K_s and R_1 upon pressure up to ~ 2 kbar was observed, it was concluded that no fine structure in the DOS of *s* character exist in the studied *i* alloy. In another NMR study of Al-Cu-Fe, Al-Cu-Ru, and Al-Pd-Re *i* QCs (Tang et al. 1997), the T^2 dependence of R_1 between 93 and 400 K, which was established on the basis of a fit of fewer than 10 experimental points, was interpreted as a signature of a sharp feature in the DOS at E_F whose width was estimated to be ~ 20 meV. However, another NMR study on *i*-Al-Pd-Re (Gavilano et al. 1997) in the temperature range 18–300 K found a T^3 dependence of R_1 .

The coefficient β of the T^3 term of the electronic contribution to the specific heat (Wälti et al. 1998) and the coefficient A of the T^2 contribution to the magnetic susceptibility (Kobayashi et al. 1997) are a function of the first and the second derivatives of $\text{DOS}(E_F)$. Large values of these derivatives are expected if the DOS has a spiky structure, which would lead to large values of β and A . This has not been observed experimentally (Kobayashi et al. 1997, Wälti et al. 1998).

A universal linear relation between $1/\rho(300\text{ K})$ and γ^2 for many *i* QCs has been found independently by Rapp (Fig. 5.10 in Chap. 5) and Mizutani (1998). This relation indicates that $1/\rho$ is proportional to the square of the $\text{DOS}(E_F)$. The fact that the experimental data on the ρ - γ diagram lie on a straight line with a slope of -2 was interpreted as evidence that the DOS around E_F must be smooth. If this was not the case, i.e., if the DOS exhibited a fine spiky structure, the data on this diagram would be scattered and no universal relation could be observed (Mizutani 1998).

It can be concluded that there is no experimental evidence based on the the high-energy-resolution PES and TS experiments which probe the DOS directly, as well as on the experiments which probe the DOS indirectly [except the claim by Tang et al. (1997)], for the presence of the predicted DOS spikiness in QCs. The possible reasons for this are discussed in Sect. 8.4.

8.4 Uniqueness of the Electronic Structure of Quasicrystals

The major effort in the theoretical and experimental investigations of the physical properties of QCs has been directed to finding the properties arising from the quasiperiodicity itself. They were expected to be different from the corresponding properties of crystalline and amorphous solids, and thus unique to QCs. Have such properties been found?

A pseudogap in the DOS around E_F predicted by theory for many non-magnetic QCs was found experimentally in some of them. It thus seems to be a generic property of the electronic structure of nonmagnetic QCs. In magnetically ordered QCs (see Chap. 9), such a pseudogap probably does not occur as a local Stoner criterion, which seems to be valid in QCs (Hafner and Krajčí 1998), requires a high DOS(E_F) for magnetic moment formation. The minimum of DOS in the vicinity of E_F is not, however, a unique characteristic which distinguishes the electronic structure of QCs from that of crystalline and amorphous alloys since the structure-induced pseudogap is believed to exist in both crystalline (Carlsson and Meschter 1995, Trambly de Laissardière et al. 1995b) and amorphous (Häussler 1994) systems.

The predicted DOS spikiness would seem to be such a unique property distinguishing QCs from other materials. The only crystalline material for which such a fine DOS structure was predicted is the cubic Al₁₀V alloy (Trambly de Laissardière et al. 1995b), but no experimental attempts have been reported yet to verify this prediction. In the discussion below several possible reasons are suggested to explain the failure to detect the DOS spikiness in QCs in various experiments probing the DOS directly and indirectly.

It has been argued (Tang et al. 1998, see also Chap. 7) that PES and TS, as surface-sensitive techniques, probe the surface electronic states of QCs rather than those of the bulk, and therefore may be not representative of the bulk DOS. Since TS probes the top-most atomic layer of a studied material, the conductance spectra reflect the surface DOS (Wolf 1985, Lang 1986, Stroscio and Kaiser 1993) which, depending on the material, may substantially differ from the bulk DOS. It is thus conceivable that the narrow (~ 60 meV wide) pseudogap observed in the TS spectra of *i* alloys (Fig. 8.7) is the gap of the surface DOS. This would be consistent with the recent theoretical results indicating that the pseudogap persists also on the surface of a QC (Janssen and Fasolino 1998). The failure to detect the predicted bulk DOS spikes ~ 10 meV wide in the vicinity of E_F in TS experiments could indicate that the DOS spikiness does not extend to the surface of a QC.

PES, on the other hand, probes deeper into the surface. The so-called “universal curve” of the electron mean-free path, λ , as a function of electron E_{kin} , which defines the surface sensitivity of the technique, has a minimum at a E_{kin} of ~ 100 eV corresponding to a λ of $\sim 5\text{--}10$ Å; the value of λ increases to ~ 20 Å for lower (~ 10 eV) and higher (~ 1000 eV) electron E_{kin} 's (Cardona and Ley 1978, Mehlhorn 1982, Hüfner 1996). This should be

compared with the diameter $\sim 8\text{--}10 \text{ \AA}$ of the elementary clusters observed in a single-grain *i*-Al-Pd-Mn alloy by scanning tunneling microscopy (Ebert et al. 1996). By changing the value of $h\nu$, one can thus vary the weight of the surface and bulk DOS contributions to the measured PES spectrum. The small λ makes thus PES a surface-sensitive technique, but not to the exclusion of the bulk response. A pseudogap an order of magnitude wider than that found in TS experiments was observed in PES experiments carried out for different values of $h\nu$, as well as by IPES, SXE, SXA, and EELS experiments (see Sect. 8.3). It thus seems that these PES experiments probe deeply enough so that they reflect mainly the bulk DOS. Additional experimental support for this statement comes from good agreement between the shape and position of different features of the PES DOS and those of the DOS predicted by theory. It should be mentioned that differences between more surface-like DOS obtained from TS experiments and more bulk-like DOS determined from PES experiments were observed for other materials (Shih et al. 1989, Takahashi 1989).

Another possible reason to explain the failure of detecting DOS spikiness in high- and ultrahigh-energy-resolution PES experiments is related to the quality of the surfaces of QCs studied. In the preparation of surfaces for these experiments by using a standard procedure of scraping or fracturing (carried out at low temperatures to prevent any structural reorganization of the sample) the polyquasicrystalline samples could, in principle, lead to a destruction of their quasicrystalline order, and thus the disappearance of the fine structure of the DOS. However, the valence bands of well-characterized single-grain *i*-Al-Pd-Mn alloys (Wu et al. 1995, Neuhold et al. 1998, Purdie et al. 1998) are virtually indistinguishable from those of polyquasicrystalline alloys (Stadnik et al. 1996, 1997), which indicates that the employed surface preparation procedures maintained the sample surface quasicrystallinity.

It may not be possible to detect the predicted DOS spikiness even with the PES experiments of the highest energy resolution because of the existence of chemical and topological disorder in QCs of high structural quality. Such disorder, which is not taken into account in the electronic structure calculations, may wash out the DOS spikiness induced by quasiperiodicity. Furthermore, the concept of quasiperiodicity implies that no two crystallographic positions of a given atom are exactly the same, which can be viewed as a sort of topological disorder. There is growing experimental evidence which shows that the chemical and topological disorder are present in these structurally "perfect" QCs. Diffuse scattering is often observed in x-ray-, electron-, and neutron-diffraction patterns of high-quality QCs (de Boissieu et al., 1995, Frey 1997, Frey et al. 1998, Mori et al. 1998). Its presence indicates that some disorder must exist in the diffracting structure. Local probes, such as Mössbauer spectroscopy (Stadnik 1996), NMR (Shastri et al. 1994b, Gavilano et al. 1997), and nuclear quadrupole resonance (Shastri et al. 1994a, 1994b), clearly detect the distribution of the electric quadrupole splittings, $P(\Delta)$,

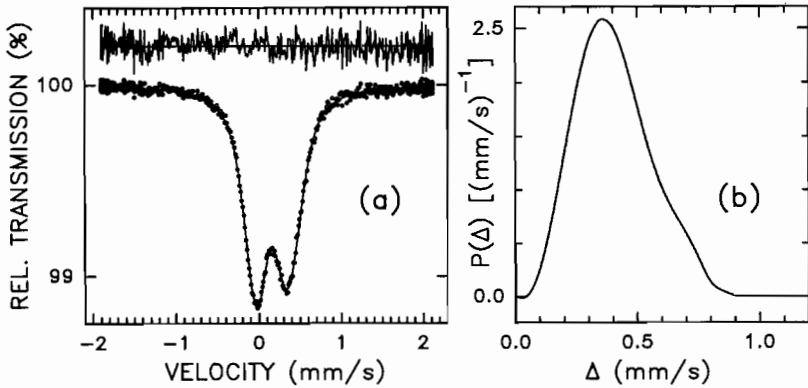


Fig. 8.21. ${}^{57}\text{Fe}$ room-temperature Mössbauer spectrum of $i\text{-Al}_{70.5}\text{Pd}_{21}\text{Re}_{8.45}\text{Fe}_{0.05}$ (a). The solid line is the fit with a distribution of quadrupole splittings $P(\Delta)$ (b). The residuals, multiplied by a factor of three, are shown above the spectrum. After Stadnik (1996).

in high-quality stable QCs. This is illustrated in Fig. 8.21a which shows a Mössbauer spectrum of the $i\text{-Al}_{70.5}\text{Pd}_{21}\text{Re}_{8.45}\text{Fe}_{0.05}$ alloy of high structural quality which consists of two broad lines. These broad lines result from the presence of the distribution $P(\Delta)$ (Fig. 8.21b). Such a distribution can be detected only if there is a chemical and/or topological order in the investigated samples (Stadnik 1996). The apparent success of quantum interference theories (the electron-electron interaction and weak-localization effects), which were originally developed for highly disordered conductors, in accounting for the temperature and field dependencies of σ and magnetoresistance of high-quality QCs (see Chap. 5) also indicates the importance of chemical disorder. The experiments mentioned above demonstrate that chemical and/or topological disorder is present in the high-quality phason-free stable QCs and therefore may smear out the DOS spikiness predicted for disorder-free QCs.

And finally, it is conceivable that the predicted DOS spikiness is an artifact of the calculations. It has been recently demonstrated (Haerle and Kramer 1998) that unphysical spikes do appear in the calculated DOS of a toy model with an assumed *a priori* smooth DOS as a result of insufficient computational precision necessary for analyzing structures with large unit cells. It was concluded that the predicted fine structure at the level of ~ 100 meV may be an artifact. This is rather an alarming possibility and it is important to investigate it in more detail. The prediction of the DOS spikiness for a cubic Al_{10}V (Trambly de Laissardière et al. 1995b) with a large lattice constant of 14.492 Å, but not for other Al-based crystalline alloys of smaller lattice constants, would seem to be in line with the conclusion that DOS spikiness is an artifact (Haerle and Kramer 1998).

The third novel electronic property intrinsic to quasiperiodicity is the concept of critical eigenstates. Whereas in periodic and random systems the

eigenstates are respectively extended and localized, they are critical in the quasiperiodic systems (see Chaps. 6 and 7), i.e., neither extended nor localized. It is not clear how these novel eigenstates reflect upon various measured physical properties. In an ^{27}Al NMR study of $i\text{-Al}_{70}\text{Pd}_{21.4}\text{Re}_{8.6}$ (Gavilano et al. 1997), a gradual localization of the itinerant electrons, which was deduced from an unusual increase of R_1/T with decreasing T below 20 K, was suggested to give, for the first time, direct evidence for the presence of critical electronic states in a QC. Further experimental studies are needed to conclusively establish the reality of the critical states in QCs.

8.5 Quasiperiodicity and Unusual Physical Properties

The electronic structure results discussed above show no unusual features that could be the consequence of the quasiperiodic order. Many unusual physical properties of QCs were also found in the approximants to QCs. For example, very high values of ρ , and its increase with temperature, were found in the approximants to the $i\text{-Mg-Ga-Al-Zn}$, $i\text{-Al-Cu-Fe}$, and $i\text{-Al-Mn-Si}$ phases (Edagawa et al. 1992, Poon 1992, Mayou et al. 1993, Pierce et al. 1993b, Takeuchi 1994, Berger et al. 1995a, 1995b) and in several d approximants along the pseudoquasiperiodic planes (Volkov and Poon 1995). Similarities were also observed between the values and/or temperature and/or magnetic field dependencies of the Hall coefficient (Berger et al. 1995b, Pierce et al. 1995b), thermoelectric power (Pierce et al. 1995b), magnetoresistance (Berger et al. 1995b), optical conductivity (Wu et al. 1993), γ (Mizutani et al. 1991, Pierce et al. 1993b, Berger et al. 1995b), and local hyperfine parameters (Hippert et al. 1992, 1994, Stadnik 1996).

The unexpectedly high value of ρ of many i alloys, which consist of normal metallic elements (see Chap. 5), was thought to be indicative of their unique properties induced by their quasiperiodic structure. But as mentioned above, similarly high values of ρ were observed in approximants to QCs. Furthermore, high ρ and its negative temperature coefficient were also observed in some crystalline alloys consisting of normal metallic elements whose structure is unrelated to the structure of QCs. For example, the Heusler-type Fe_2VAl alloy exhibits a semiconductor-like behavior of ρ (Fig. 8.22a), yet its valence band (Fig. 8.22b) clearly shows the presence of the Fermi edge. Electronic structure calculations predict a narrow pseudogap in the DOS around E_F (Guo et al. 1998, Singh and Mazin 1998).

It has to be concluded that, as yet, no conclusive experimental evidence has been found to support the claim of the unusual physical properties of QCs which are due to their quasiperiodic nature and which therefore do not occur in crystalline or amorphous systems. This is perhaps not surprising since there is no solid physical basis to expect that quasiperiodicity should lead to physical properties distinctly different from those found in periodic systems.

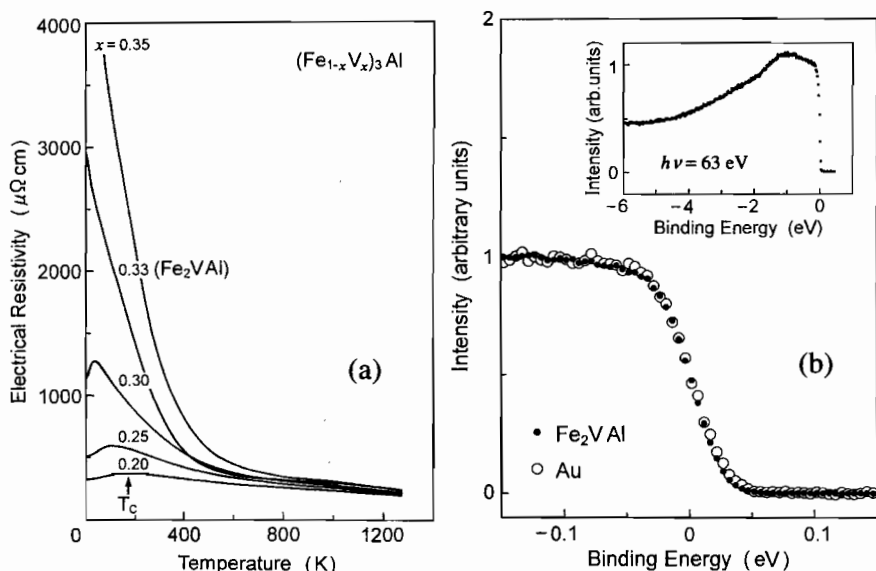


Fig. 8.22. (a) Temperature dependence of electrical resistivity in $(\text{Fe}_{1-x}\text{V}_x)_3\text{Al}$ with $0.20 \leq x \leq 0.35$. The arrow indicates the Curie temperature. Note a semiconductor-like behavior of Fe_2VAl ($x = 0.33$). (b) Near- E_F PES spectra of Fe_2VAl (full circles) and Au (open circles). The inset shows the valence band of Fe_2VAl . The spectra were measured at 40 K and with $h\nu = 63$ eV. After Nishino et al. (1997).

8.6 Conclusions and Outlook

Experimental results obtained with main spectroscopic methods on the electronic structure of QCs were reviewed. Generally good agreement was observed between the overall structure of the calculated DOS for approximants to QCs and that determined experimentally. The presence of a pseudogap in the DOS was conclusively shown to exist in a few i alloys. Some evidence for its presence exists for d alloys. The theoretically predicted DOS spikiness was not observed experimentally. Various possible reasons for this were considered, including the possibility that the fine structure of DOS is an artifact of calculations. No physical properties of QCs could be identified as resulting directly from their quasiperiodic nature; similar properties are found in crystalline alloys.

The issue of DOS spikiness in QCs is an outstanding problem. On a theoretical side, an effort should be made to establish that DOS spikiness is not an artifact. On the experimental side, near- E_F spectroscopic studies with high energy resolution probing bulk electronic states are necessary to resolve the issue of the DOS spikiness. As more QCs in a single-grain form become available, their surface DOS becomes of interest and theoretical calculations are needed to establish how it differs from the bulk DOS. With single-grain

QCs of high purity, the de Haas–van Alphen effect experiments become feasible; they could conclusively verify the existence and the details of the Fermi surface in QCs.

Acknowledgment

This work was supported by the Natural Sciences and Engineering Research Council of Canada.

References

- Agarwal, B.K. (1991): X-Ray Spectroscopy, 2nd ed. Springer-Verlag, Berlin
- Ahlgren, M., Gignoux, C., Rodmar, M., Berger, C., Rapp, Ö (1997): *Phys. Rev. B* **55**, R11 915
- Bancel, P.A., Heiney, P.A. (1986): *Phys. Rev. B* **33**, 7917
- Belin, E., Mayou, D. (1993): *Phys. Scr. T* **49**, 356
- Belin, E., Dankhazi, Z., Sadoc, A. (1993): *J. Non-Cryst. Solids* **156-158**, 896
- Belin, E., Dankházi, Z., Sadoc, A., Dubois, J.M. (1994a): *J. Phys. Condens. Matter* **6**, 8771
- Belin, E., Dankhazi, Z., Sadoc, A., Dubois, J.M., Calvayrac, Y. (1994b): *Europhys. Lett.* **26**, 677
- Berger, C., Mayou, D., Cyrot-Lackmann, F. (1995a): in *Proceedings of the 5th International Conference on Quasicrystals*, Janot, C., Mosseri, R. (eds). World Scientific, Singapore, p 423
- Berger, C., Gignoux, C., Tjernberg, O., Lindqvist, P., Cyrot-Lackmann, F., Calvayrac, Y. (1995b): *Physica B* **204**, 44
- Bianchi, A.D., Chernikov, M.A., Beeli, C., Ott, H.R. (1993): *Solid State Commun.* **87**, 721
- Bianchi, A.D., Bommeli, F., Chernikov, M.A., Gubler, U., Degiorgi, L., Ott, H.R. (1997): *Phys. Rev. B* **55**, 5730
- Bianchi, A.D., Bommeli, F., Felder, E., Kenzelmann, M., Chernikov, M.A., Degiorgi, L., Ott, H.R. (1998): *Phys. Rev. B* **58**, 3046
- Burkov, S.E. (1991): *Phys. Rev. Lett.* **67**, 614
- Cardona, M., Ley, L. (eds) (1978): *Photoemission in Solids I*. Springer-Verlag, Berlin
- Carlsson, A.E., Meschter, P.J. (1995): in *Intermetallic Compounds*, Vol. 1, Westbrook, J.H., Fleischer, R.L. (eds). John Wiley and Sons, Chichester, p 55
- Davydov, D.N., Mayou, D., Berger, C., Gignoux, C., Neumann, A., Jansen, A.G.M., Wyder, P. (1996): *Phys. Rev. Lett.* **77**, 3173
- de Boissieu, M., Boudard, M., Hennion, B., Bellissent, R., Kycia, S., Goldman, A., Janot, C., Audier, M. (1995): *Phys. Rev. Lett.* **75**, 89
- Dell'Acqua, G., Krajić, M., Hafner, J. (1997): *J. Phys. Condens. Matter* **9**, 10 725
- Depero, L.E., Parmigiani, F. (1993): *Chem. Phys. Lett.* **214**, 208
- Dubost, B., Lang, J.-M., Tanaka, M., Sainfort, P., Audier, M. (1997): *Nature* **324**, 48
- Ebert, Ph., Feuerbacher, M., Tamura, N., Wollgarten, M., Urban, K. (1996): *Phys. Rev. Lett.* **77**, 3827
- Edagawa, K., Naiti, N., Takeuchi, S. (1992): *Philos. Mag. B* **65**, 1011

- Frey, F. (1997): *Z. Kristallogr.* **212**, 257
- Frey, F., Hradil, K., Grushko, B., McIntyre, G.J. (1998): in *Proceedings of the 6th International Conference on Quasicrystals*, Takeuchi, S., Fujiwara, T. (eds). World Scientific, Singapore, p 37
- Friedel, J., Dénoyer, F. (1987): *C.R. Acad. Sci. Paris* **305**, 171
- Friedel, J. (1988): *Helv. Phys. Acta* **61**, 538
- Friedel, J. (1992): *Philos. Mag. B* **65**, 1125
- Fuggle, J.C., Inglesfield, J.E. (eds) (1992): *Unoccupied Electronic States*. Springer-Verlag, Berlin
- Fujiwara, T. (1989): *Phys. Rev. B* **40**, 942
- Fujiwara, T. (1997): unpublished
- Fujiwara, T. (1998): in *Proceedings of the 6th International Conference on Quasicrystals*, Takeuchi, S., Fujiwara, T. (eds). World Scientific, Singapore, p 591
- Fujiwara, T., Yokokawa, T. (1991): *Phys. Rev. Lett.* **66**, 333
- Fujiwara, T., Yamamoto, S., Trambly de Laissardière, G. (1993): *Phys. Rev. Lett.* **71**, 4166
- Gavilano, J.L., Ambrosini, B., Vonlanthen, P., Chernikov, M.A., Ott, H.R. (1997): *Phys. Rev. Lett.* **79**, 3058
- Guo, G.Y., Botton, G.A., Nishino, Y. (1998): *J. Phys. Condens. Matter* **10**, L119
- Haerle, R., Kramer, P. (1998): *Phys. Rev. B* **58**, 716
- Hafner, J., Krajčí, M. (1992): *Phys. Rev. Lett.* **68**, 2321
- Hafner, J., Krajčí, M. (1993): *Phys. Rev. B* **47**, 11 795
- Hafner, J., Krajčí, M. (1998): *Phys. Rev. B* **57**, 2849
- Haanappel, E.G., Rabson, D.A., Mueller, F.M. (1996): in *Proceedings of Physical Phenomena at High Magnetic Fields - II*, Fisk, Z., Gor'kov, L., Meltzer, D., Schrieffer, R. (eds). World Scientific, Singapore, p 362
- Häussler, P. (1994): in *Glassy Metals III*, Beck, H., Güntherodt, H.-J. (eds). Springer-Verlag, Berlin, p 163
- Hennig, R.G., Teichler, H. (1997): *Philos. Mag. A* **76**, 1053
- Hippert, F., Kandel, L., Calvayrac, Y., Dubost, B. (1992): *Phys. Rev. Lett.* **69**, 2086
- Hippert, F., Brand, R.A., Pelloth, J., Calvayrac, Y. (1994): *J. Phys. Condens. Matter* **6**, 11 189
- Hüfner, S. (1996): *Photoelectron Spectroscopy*, 2nd ed. Springer-Verlag, Berlin
- Inoue, A., Tsai, A.-P., Masumoto, T. (1990): in *Quasicrystals*, Fujiwara, T., Ogawa, T. (eds). Springer-Verlag, Berlin, p 80
- Janssen, T., Fasolino, A. (1998): in *Proceedings of the 6th International Conference on Quasicrystals*, Takeuchi, S., Fujiwara, T. (eds). World Scientific, Singapore, p 757
- Kirihara, K., Kimura, K., Ino, H., Kumigashira, H., Ashihara, A., Takahashi, T. (1998): in *Proceedings of the 6th International Conference on Quasicrystals*, Takeuchi, S., Fujiwara, T. (eds). World Scientific, Singapore, p 651
- Klein, T., Symko, O.G., Davydov, D.N., Jansen, A.G.M. (1995): *Phys. Rev. Lett.* **74**, 3656
- Knapp, J.A., Himpsel, F.J., Eastman, D.E. (1979): *Phys. Rev. B* **19**, 4952
- Kobayashai, A., Matsuo, S., Ishimasa, T., Nakano, H. (1997): *J. Phys. Condens. Matter* **9**, 3205
- Kortboyer, S.W., Grioni, M., Speier, W., Zeller, R., Watson, L.M., Gibson, M.T., Schäfers, F., Fuggle, J.C. (1989): *J. Phys. Condens. Matter* **1**, 5981
- Krajčí, M., Hafner, J. (1994): *Europhys. Lett.* **27**, 147
- Krajčí, M., Hafner, J. (1998): unpublished

- Krajčí, M., Windisch, M., Hafner, J., Kresse, G., Mihalkovič, M. (1995): *Phys. Rev. B* **51**, 17 355
- Krajčí, M., Hafner, J., Mihalkovič, M. (1996): *Europhys. Lett.* **34**, 207
- Krajčí, M., Hafner, J., Mihalkovič, M. (1997a): *Phys. Rev. B* **56**, 3072
- Krajčí, M., Hafner, J., Mihalkovič, M. (1997b): *Phys. Rev. B* **55**, 843
- Lang, N.D. (1986): *Phys. Rev. B* **34**, 5947
- Ley, L., Cardona M., (eds) (1979): *Photoemission in Solids II*. Springer-Verlag, Berlin
- Matsubara, H., Ogawa, S., Kinoshita, T., Kishi, K., Takeuchi, S., Kimura, K., Suga, S. (1991): *Jpn. J. Appl. Phys. A* **30**, L389
- Mayou, D., Berger, C., Cyrot-Lackmann, F., Klein, T., Lanco, P. (1993): *Phys. Rev. Lett.* **70**, 3915
- Mehlhorn, W. (ed) (1982): *Corpuscles and Radiation in Matter I*. Springer-Verlag, Berlin
- Mizutani, U. (1998): *J. Phys. Condens. Matter* **10**, 4609
- Mizutani, U., Kamiya, A., Matsuda, T., Kishi, K., Takeuchi, S. (1991): *J. Phys. Condens. Matter* **3**, 3711
- Mizutani, U., Matsuda, T., Itoh, Y., Tanaka, K., Domae, H., Mizuno, T., Murasaki, S., Miyoshi, Y., Hashimoto, K., Yamada, Y. (1993): *J. Non-Cryst. Solids* **156-158**, 882
- Mizutani, U., Iwakami, W., Fujiwara, T. (1998): in *Proceedings of the 6th International Conference on Quasicrystals*, Takeuchi, S., Fujiwara, T. (eds). World Scientific, Singapore, p 579
- Mori, M., Matsuo, S., Ishimasa, T., Matsuura, T., Kamiya, K., Inokuchi, H., Matsukawa, T. (1991): *J. Phys. Condens. Matter* **3**, 767
- Mori, M., Kamiya, K., Matsuo, S., Ishimasa, T., Nakano, H., Fujimoto, H., Inokuchi, H. (1992): *J. Phys. Condens. Matter* **4**, L157
- Mori, M., Ogawa, T., Ishimasa, T., Tanaka, M., Sasaki, S. (1998): in *Proceedings of the 6th International Conference on Quasicrystals*, Takeuchi, S., Fujiwara, T. (eds). World Scientific, Singapore, p 387
- Neuhold, G., Barman, S.R., Horn, K., Theis, W., Ebert, P., Urban, K. (1998): *Phys. Rev. B* **58**, 734
- Nishino, Y., Kato, M., Asano, S., Soda, K., Hayasaki, M., Mizutani, U. (1997): *Phys. Rev. Lett.* **79**, 1909
- Pierce, F.S., Poon, S.J., Guo, Q. (1993a): *Science* **261**, 737
- Pierce, F.S., Bancel, P.A., Biggs, B.D., Guo, Q., Poon, S.J. (1993b): *Phys. Rev. B* **47**, 5670
- Pierce, F.S., Guo, Q., Poon, S.J. (1994): *Phys. Rev. Lett.* **73**, 2220
- Poon, S.J. (1992): *Adv. Phys.* **41**, 303
- Purdie, D., Garnier, M., Hengsberger, M., Baer, Y., Stadnik, Z.M., Lograsso, T.A., Delaney, D.W. (1998): unpublished
- Roche, S., Trambly de Laissardière, G., Mayou, D. (1997): *J. Math. Phys.* **38**, 1794
- Sabiryanov, R.F., Bose, S.K. (1994): *J. Phys. Condens. Matter* **6**, 6197; Erratum (1995) **7**, 2375
- Sabiryanov, R.F., Bose, S.K., Burkov, S.E. (1995): *J. Phys. Condens. Matter* **7**, 5437
- Sadoc, A., Belin, E., Dankhazi, Z., Flank, A.M. (1993): *J. Non-Cryst. Solids* **153-154**, 338
- Shastri, A., Borsa, F., Torgeson, D.R., Goldman, A.I. (1994a): *Phys. Rev. B* **50**, 4224
- Shastri, A., Borsa, F., Torgeson, D.R., Shield, J.E., Goldman, A.I. (1994b): *Phys. Rev. B* **50**, 16651

- Shastri, A., Baker, D.B., Conradi, M.S., Borsa, F., Torgeson, D.R. (1995): *Phys. Rev. B* **52**, 12681
- Shechtman, D., Blech, I., Gratias, D., Cahn, J.W. (1984): *Phys. Rev. Lett.* **53**, 1951
- Shih, C.K., Feenstra, R.M., Kirtley, J.R., Chandrashekar, G.V. (1989): *Phys. Rev. B* **40**, 2682
- Singh, D.J., Mazin, I.I. (1998): *Phys. Rev. B* **57**, 14352
- Shoenberg, D. (1984): *Magnetic Oscillations in Metals*. Cambridge University Press, New York
- Smith, A.P., Ashcroft, N.W. (1987): *Phys. Rev. Lett.* **59**, 1365
- Soda, K., Nozawa, K., Yanagida, Y., Morita, K., Mizutani, U., Yokoyama, Y., Note, R., Inoue, A., Ishii, H., Tezuka, Y., Shin, S., (1998a): *J. Electron Spectrosc. Relat. Phenom.* **88-91**, 415
- Soda, K., Mizutani, U., Yokoyama, Y., Note, R., Inoue, A., Fujisawa, M., Shin, S., Suga, S., Sekiyama, A., Susaki, T., Konishi, T., Matsushita, T., Miyahara, T. (1998b): in *Proceedings of the 6th International Conference on Quasicrystals*, Takeuchi, S., Fujiwara, T. (eds). World Scientific, Singapore, p 676
- Stadnik, Z.M. (1996): in *Mössbauer Spectroscopy Applied to Magnetism and Materials Science*, Vol. 1, Long, G.J., Grandjean, F. (eds). Plenum, New York, p 125
- Stadnik, Z.M., Stroink, G., (1993): *Phys. Rev. B* **47**, 100
- Stadnik, Z.M., Purdie, D. (1997): unpublished
- Stadnik, Z.M., Zhang, G.W., Tsai, A.-P., Inoue, A. (1995a): *Phys. Rev. B* **51**, 4023
- Stadnik, Z.M., Zhang, G.W., Tsai, A.-P., Inoue, A. (1995b): in *Proceedings of the 5th International Conference on Quasicrystals*, Janot, C., Mosseri, R. (eds). World Scientific, Singapore, p 249
- Stadnik, Z.M., Zhang, G.W., Akbari-Moghanjoughi, M., Tsai, A.-P., Inoue, A. (1995c): in *Proceedings of the 5th International Conference on Quasicrystals*, Janot, C., Mosseri, R. (eds). World Scientific, Singapore, p 530
- Stadnik, Z.M., Zhang, G.W., Tsai, A.-P., Inoue, A. (1995d): *Phys. Rev. B* **51**, 11358
- Stadnik, Z.M., Purdie, D., Garnier, M., Baer, Y., Tsai, A.-P., Inoue, A., Edagawa, K., Takeuchi, S. (1996): *Phys. Rev. Lett.* **77**, 1777
- Stadnik, Z.M., Purdie, D., Garnier, M., Baer, Y., Tsai, A.-P., Inoue, A., Edagawa, K., Takeuchi, S., Buschow, K.H.J. (1997): *Phys. Rev. B* **55**, 10938
- Stadnik, Z.M., Purdie, D., Garnier, M., Baer, Y., Tsai, A.-P., Inoue, A., Edagawa, K., Takeuchi, S. (1998): in *Proceedings of the 6th International Conference on Quasicrystals*, Takeuchi, S., Fujiwara, T. (eds). World Scientific, Singapore, p 563
- Strosio, J.A., Kaiser, W.J. (eds) (1993): *Scanning Tunneling Microscopy*. Academic, San Diego
- Takahashi (1989): in *Strong Correlation and Superconductivity*, Fukuyama, H., Maekawa, S., Malozemoff, A.P. (eds). Springer-Verlag, Berlin, p 311
- Takeuchi, S. (1994): *Mater. Sci. Forum* **150-151**, 35
- Takeuchi, T., Mizutani, U. (1995): *Phys. Rev. B* **52**, 9300
- Tang, X.-P., Hill, E.A., Wonnell, S.K., Poon, S.J., Wu, Y. (1997): *Phys. Rev. Lett.* **79**, 1070
- Terauchi, M., Tanaka, M., Tsai, A.-P., Inoue, A., Masumoto, T. (1996): *Philos. Mag. B* **74**, 107
- Terauchi, M., Ueda, H., Tanaka, M., Tsai, A.P., Inoue, A., Masumoto, T. (1998a): in *Proceedings of the 6th International Conference on Quasicrystals*, Takeuchi, S., Fujiwara, T. (eds). World Scientific, Singapore, p 587
- Terauchi, M., Ueda, H., Tanaka, M., Tsai, A.-P., Inoue, A., Masumoto, T. (1998b): *Philos. mag. Lett.* **77**, 351

- Terauchi, M., Ueda, H., Tanaka, M., Tsai, A.-P., Inoue, A., Masumoto, T. (1998c): *Philos. Mag. B* **77**, 1625
- Trambly de Laissardière, G., Fujiwara, T. (1994a): *Phys. Rev. B* **50**, 5999
- Trambly de Laissardière, G., Fujiwara, T. (1994b): *Phys. Rev. B* **50**, 9843
- Trambly de Laissardière, G., Fujiwara, T. (1994c): *Mater. Sci. Eng. A* **181-182**, 722
- Trambly de Laissardière, G., Dankházi, Z., Belin, E., Sadoc, A., Nguyen Manh, D., Mayou, D., Keegan, M.A., Papaconstantopoulos, D.A. (1995a): *Phys. Rev. B* **51**, 12035
- Trambly de Laissardière, G., Nguyen Manh, D., Magaud, L., Julien, J.P., Cyrot-Lackmann, F., Mayou, D. (1995b): *Phys. Rev. B* **52**, 7920
- Tsai, A.-P., Inoue, A., Masumoto, T. (1989a): *Mater. Trans., Jpn. Inst. Met.* **30**, 463
- Tsai, A.-P., Inoue, A., Masumoto, T. (1989b): *Mater. Trans., Jpn. Inst. Met.* **30**, 666
- Vaks, V.G., Kamyshenko, V.V., Samolyuk, G.D. (1988): *Phys. Lett. A* **132**, 131
- Volkov, P., Poon, S.J. (1995): *Phys. Rev. B* **52**, 12685
- Windisch, M., Krajčí, M., Hafner, J. (1994): *J. Phys. Condens. Matter* **6**, 6977
- Wälti, Ch., Felder, E., Chernikov, M.A., Ott, H.R., de Boissieu, M., Janot, C. (1998): *Phys. Rev. B* **57**, 10504
- Wolf, E.L. (1985): *Principles of Electron Tunneling Spectroscopy*. Oxford University Press, New York
- Wu, X., Homes, C.C., Burkov, S.E., Timusk, T., Pierce, F.S., Poon, S.J., Cooper, S.L., Karlow, A.M. (1993): *J. Phys. Condens. Matter* **5**, 5975
- Wu, X., Kycia, S.W., Olson, C.G., Benning, P.J., Goldman, A.I., Lynch, D.W. (1995): *Phys. Rev. Lett.* **75**, 4540
- Yeh, J.-J. (1993): *Atomic Calculations of the Photoionization Cross-Sections and Asymmetry Parameters*. Gordon and Breach, New York
- Zhang, G.W., Stadnik, Z.M. (1995): in *Proceedings of the 5th International Conference on Quasicrystals*, Janot, C., Mosseri, R. (eds). World Scientific, Singapore, p 552
- Zhang, G.W., Stadnik, Z.M., Tsai, A.-P., Inoue, A. (1994): *Phys. Rev. B* **50**, 6696
- Zhang, G.W., Stadnik, Z.M., Tsai, A.-P., Inoue, A., Miyazaki, T. (1995): *Z. Phys. B* **97**, 439